

# Permutation-Avoiding FFT-Based Convolution

NICOLAS VENKOVIC and HARTWIG ANZT, Computational Mathematics, School of Computation, Information and Technology, Technical University of Munich, Germany

Fast Fourier Transform (FFT) libraries are widely used for evaluating discrete convolutions. Most FFT implementations follow some variant of the Cooley-Tukey framework, in which the transform is decomposed into butterfly operations and index-reversal permutations. While butterfly operations dominate the floating-point operation count, the memory access patterns induced by index-reversal permutations significantly degrade the FFT's arithmetic intensity. In practice, discrete convolutions are often applied repeatedly with a fixed filter. In such cases, we show that the index-reversal permutations involved in both the forward and backward transforms of standard FFT-based convolution implementations can be avoided by deferring to a single offline permutation of the filter. We propose a multi-dimensional, permutation-avoiding convolution procedure within a general radix Cooley-Tukey framework. We perform numerical experiments to benchmark our algorithms against state-of-the-art FFT-based convolution implementations. Our results suggest that developers of FFT libraries should consider supporting permutation-avoiding convolution kernels.

CCS Concepts: • **Mathematics of computing** → **Mathematical software performance**; • **Software and its engineering** → *Software libraries and repositories*.

Additional Key Words and Phrases: Fast Fourier transform (FFT), Cooley-Tukey Framework, Index-Reversal Permutation, Discrete Convolution, Cache-Friendly Algorithms, C

## ACM Reference Format:

Nicolas Venkovic and Hartwig Anzt. 2025. Permutation-Avoiding FFT-Based Convolution. *ACM Trans. Math. Softw.* 1, 1 (June 2025), 38 pages. <https://doi.org/XXXXXXX.XXXXXXX>

## 1 Introduction

Discrete convolution is a prevalent kernel of numerical simulations and data processing. Example applications of discrete convolution are iterative solvers for classical physics simulation [Moulinec and Suquet 1998; Zeman et al. 2010], stationary Gaussian process simulation by circulant embedding [Chan and Wood 1997; Dietrich and Newsam 1993, 1997; Wood and Chan 1994], fast Poisson solvers [Swarztrauber 1977] as well as signal [Oppenheim 1999] and image [Gonzalez 2009] processing. One way to perform a discrete convolution is first to compute a forward discrete Fourier transform (DFT) of the data, do component-wise multiplication with the transformed filter, and then apply the inverse DFT. In practice, this is achieved using highly optimized implementations of the forward and backward fast Fourier transform (FFT), e.g., FFTW [Frigo and Johnson 1998, 2005], Intel MKL [Intel Corporation 2025], etc.

The Cooley-Tukey framework, introduced in [Cooley and Tukey 1965], fundamentally transformed discrete Fourier transform computation by reducing the complexity from  $O(n^2)$  to  $O(n \log n)$

---

Authors' Contact Information: Nicolas Venkovic, [venkovic@gmail.com](mailto:venkovic@gmail.com), [nicolas.venkovic@tum.de](mailto:nicolas.venkovic@tum.de); Hartwig Anzt, [hartwig.anzt@tum.de](mailto:hartwig.anzt@tum.de), Computational Mathematics, School of Computation, Information and Technology, Technical University of Munich, Germany.

---

Permission to make digital or hard copies of all or part of this work for personal or classroom use is granted without fee provided that copies are not made or distributed for profit or commercial advantage and that copies bear this notice and the full citation on the first page. Copyrights for components of this work owned by others than the author(s) must be honored. Abstracting with credit is permitted. To copy otherwise, or republish, to post on servers or to redistribute to lists, requires prior specific permission and/or a fee. Request permissions from [permissions@acm.org](mailto:permissions@acm.org).

© 2025 Copyright held by the owner/author(s). Publication rights licensed to ACM.

ACM 1557-7295/2025/6-ART

<https://doi.org/XXXXXXX.XXXXXXX>

through a divide-and-conquer approach. While alternative FFT algorithms exist (prime factor algorithm [Good 1958; Thomas 1963], Rader’s algorithm [Rader 1968], Bluestein’s algorithm [Bluestein 1970], four-step FFT [Bailey 1990; Gentleman and Sande 1966], split-radix FFT [Duhamel and Hollmann 1984; Yavne 1968]), the Cooley-Tukey framework remains the foundation of virtually all production FFT libraries due to its broad applicability to composite sizes  $n = r^t$ , predictable performance, and implementation simplicity. The Cooley-Tukey framework decomposes DFT computation into two distinct operations:

- **Butterfly operations:** Computational kernels with regular memory access patterns.
- **Index-reversal permutations:** Data reorganization following index-reversal patterns, where index-reversal is a generalization of bit-reversal ordering to non-binary representations.

Here, our focus is on general radix Cooley-Tukey. This choice is motivated by theoretical clarity in exposing computation-versus-data-movement trade-offs and practical relevance since insights directly translate to mixed-radix implementations used in production libraries.

While butterfly operations dominate floating-point operation count, index-reversal permutations create a fundamentally different performance bottleneck. Butterfly operations involve regular, predictable memory access patterns enabling vectorization and cache optimizations. In contrast, *index-reversal permutations require scattered memory accesses following pseudo-random patterns, creating cache misses and preventing effective vectorization.* Critically, *index-reversal permutations have zero arithmetic intensity*, consisting purely of memory movement with no floating-point arithmetic, while butterfly operations achieve high arithmetic intensity through data reuse.

Index-reversal permutation complexity scales unfavorably with problem size. For 1D FFT of size  $n = r^t$ , permutations require  $n$  memory reads and writes with stride patterns depending on radix  $r$  and depth  $t = \log_r(n)$ . *As  $n$  increases beyond cache capacity, permutations operate on main memory with significantly higher latency.*

Discrete convolutions are often applied repeatedly with fixed filters in signal processing, iterative PDE solvers, and machine learning. Traditional FFT-based convolution requires two permutation applications per evaluation, resulting in  $2M$  total permutations for  $M$  repeated evaluations. In this work, we present algorithmic contributions to perform FFT-based convolution of multi-dimensional data in a way that minimizes index-reversal permutations. Our permutation-avoiding approach reduces the number of index-reversal permutation of a convolution to a single offline filter permutation during preprocessing, followed by an entirely permutation-free online evaluation of unordered forward and backward FFTs.

This paper is organized as follows. Section 2 presents the 1D problem, Section 3 extends to 2D, and Section 4 covers the general multi-dimensional case. Section 5 presents our algorithms and implementation details of the C code we developed in this study which is available at the following address:

<https://github.com/venkovic/c-permutation-avoiding-convolution>.

Section 6 provides experimental results, and Section 7 discusses practical implications including applicability to other FFT frameworks. Finally, the conclusions of this work are presented in Section 8.

## 2 1D problem

The discrete Fourier transform (DFT) can be defined as

$$\begin{aligned} \text{DFT}_n : \mathbb{C}^n &\rightarrow \mathbb{C}^n \\ x &\mapsto F_n x \end{aligned} \tag{1}$$

where  $F_n \in \mathbb{C}^{n \times n}$  is a Fourier matrix with components  $(F_n)_{jk} = \omega_n^{j \cdot k}$  in which

$$\omega_n := \exp(-2\pi i/n) \quad (2)$$

and where  $i$  is the imaginary number. The DFT being an invertible procedure, we have

$$\begin{aligned} \text{DFT}_n^{-1} : \mathbb{C}^n &\rightarrow \mathbb{C}^n \\ h &\mapsto F_n^{-1}h. \end{aligned} \quad (3)$$

Beyond the DFT, we are particularly interested in the function

$$\begin{aligned} \mathcal{F}_g : \mathbb{C}^n &\rightarrow \mathbb{C}^n \\ x &\mapsto \text{DFT}_n^{-1}(\text{diag}(g) \cdot \text{DFT}_n(x)) \end{aligned} \quad (4)$$

for some  $g \in \mathbb{C}^n$ , where  $\text{diag}(g)$  denotes the  $n \times n$  diagonal matrix with components of  $g$  on the diagonal. When  $g = \text{DFT}_n(h)$  for some  $h \in \mathbb{C}^n$ , we say that  $\mathcal{F}_g(x)$  is the discrete convolution of  $x$  with  $h$ , which is sometimes written as  $h * x$ .

## 2.1 General radix Cooley-Tukey framework

Several frameworks exist for formulating the FFT, the most common of which are based on variants of the approach introduced by James William Cooley and John Tukey [Cooley and Tukey 1965], such as general radix, mixed radix, and split-radix algorithms. The Cooley-Tukey framework recursively decomposes a discrete Fourier transform (DFT) of composite size into smaller DFTs, achieving a computational complexity of  $O(n \log n)$ . Because it reduces the DFT into smaller subproblems, Cooley-Tukey can be combined with other DFT algorithms, such as Rader's or Bluestein's methods, to handle large prime sizes, or with the prime factor algorithm to exploit relatively prime factorizations more efficiently. Moreover, the Cooley-Tukey method naturally admits a matrix-based formulation, which we present below, as it proves useful in describing our proposed method. A good reference for what is presented below is the book of [Van Loan 1992].

If  $n$  is a power of  $r$ , i.e.,  $n = r^t$  for some positive integer  $t$ , then we can resort to the general radix- $r$  Cooley-Tukey factorization of the Fourier matrix, i.e., we have

$$F_n = A_{r,n} P_{r,n} \quad (5)$$

in which  $A_{r,n} \in \mathbb{C}^{n \times n}$  is a product of block butterfly matrices, i.e.,

$$A_{r,n} = B_{r,t,n} B_{r,t-1,n} \dots B_{r,2,n} B_{r,1,n} \quad \text{where } t := \log_r n \quad (6)$$

with block butterfly matrices given by

$$B_{r,q,n} = I_{\frac{n}{r^q}} \otimes B_{r,r^q} = \underbrace{\text{diag}(B_{r,r^q}, \dots, B_{r,r^q})}_{\frac{n}{r^q} \text{ times}} \quad \text{for } 1 \leq q \leq t, \quad (7)$$

and  $P_{r,n} \in \mathbb{R}^{n \times n}$  is a symmetric index-reversal permutation matrix, i.e.,  $P_{r,n} = P_{r,n}^T = P_{r,n}^{-1}$ .

For any  $n$  which is a power of  $r$ , the  $n \times n$  butterfly matrix denoted by  $B_{r,n}$  is given by

$$B_{r,n} = (F_r \otimes I_{n/r}) \cdot \text{diag}\left(I_{n/r}, \Omega_{r,n/r}, \Omega_{r,n/r}^2, \dots, \Omega_{r,n/r}^{r-1}\right) \quad (8)$$

where

$$\Omega_{r,n} = \text{diag}\left(1, \omega_{rn}, \omega_{rn}^2, \dots, \omega_{rn}^{n-1}\right). \quad (9)$$

For example, in the radix-2 case, it is well-known that Eq. (8) simplifies to

$$B_{2,n} = \begin{bmatrix} I_{n/2} & \Omega_{n/2} \\ I_{n/2} & -\Omega_{n/2} \end{bmatrix}. \quad (10)$$

The index-reversal permutation matrix denoted by  $P_{r,n} \in \mathbb{R}^{n \times n}$  is given by

$$P_{r,n} = R_{r,t,n} R_{r,t-1,n} \dots R_{r,2,n} R_{r,1,n} \quad (11)$$

where each permutation matrix  $R_{r,q,n}$  is of the form

$$R_{r,q,n} = I_{r^{q-1}} \otimes R_{r,n/r^{q-1}} = \underbrace{\text{diag}(R_{r,n/r^{q-1}}, \dots, R_{r,n/r^{q-1}})}_{r^{q-1} \text{ times}} \quad (12)$$

in which  $R_{r,n/r^{q-1}}$  is a modulo  $r$  sort permutation matrix. That is, for any  $n$  which is a power of  $r$ ,  $R_{r,n}$  is such that

$$R_{r,n}x = [x_1, x_{r+1}, x_{2r+1}, \dots, x_{n-r+1}, x_2, x_{r+2}, x_{2r+2}, \dots, x_{n-r+2}, \dots, x_r, x_{2r}, x_{3r}, \dots, x_n]^T \quad (13)$$

for all  $x \in \mathbb{C}^n$ . This operation groups elements by their residue modulo- $r$ , effectively performing a radix- $r$  digit-based reordering. The modulo- $r$  sorting generalizes the even-odd sorting from the radix-2 case in the context of zero-based indexing.

Note that, by symmetry of the Fourier matrix, we have

$$F_n = F_n^T = (A_{r,n} P_{r,n})^T = P_{r,n}^T A_{r,n}^T = P_{r,n} A_{r,n}^T. \quad (14)$$

It is also well known (e.g., see [Van Loan 1992]) that

$$F_n^{-1} = \overline{F_n}/n = \overline{A_{r,n} P_{r,n}}/n = \overline{A_{r,n}} P_{r,n}/n. \quad (15)$$

## 2.2 Permutation-avoiding 1D convolution

Using the factorizations  $F_n = P_{r,n} A_{r,n}^T$  and  $F_n^{-1} = \overline{A_{r,n}} P_{r,n}/n$  in the matrix form of Eq. (4), we obtain

$$\mathcal{F}_g(x) = F_n^{-1} \text{diag}(g) F_n x = \overline{A_{r,n}} P_{r,n} \text{diag}(g) P_{r,n} A_{r,n}^T x/n. \quad (16)$$

But since  $P_{r,n}$  is a symmetric permutation matrix, we have  $P_{r,n} \text{diag}(g) P_{r,n} = \text{diag}(P_{r,n} g)$ , and we can write

$$\mathcal{F}_g(x) = \overline{A_{r,n}} \text{diag}(\widehat{g}) A_{r,n}^T x/n \quad (17)$$

where

$$\widehat{g} := P_{r,n} g. \quad (18)$$

Alternatively, we write

$$\mathcal{F}_g(x) = \overline{A_{r,n}} (\widehat{g} \circ (A_{r,n}^T x))/n \quad (19)$$

in which  $\circ$  denotes the Hadamard, i.e., component-wise product. Eq. (19) is what we refer to as the permutation-avoiding 1D convolution of  $x$  with some  $h$  such that  $g = \text{DFT}_n(h)$ , i.e.,  $h * x$ . In a scenario where  $g$  is fixed and one wishes to evaluate  $\mathcal{F}_g$  for a sequence of inputs  $x_1, x_2, \dots \in \mathbb{C}^n$ ,  $\widehat{g}$  is constructed offline, and the online evaluation of  $\mathcal{F}_g$  after Eq. (19) is index-reversal-free, whereas a standard FFT-based evaluation of the convolution would require *two applications of the index-reversal permutation per evaluation of  $\mathcal{F}_g$* .

## 3 2D problem

The 2D DFT can be defined as

$$\begin{aligned} \text{DFT}_{n_1 \times n_2} : \mathbb{C}^{n_1 \times n_2} &\rightarrow \mathbb{C}^{n_1 \times n_2} \\ X &\mapsto F_{n_1} X F_{n_2} \end{aligned} \quad (20)$$

with an inverse given by

$$\begin{aligned} \text{DFT}_{n_1 \times n_2}^{-1} : \mathbb{C}^{n_1 \times n_2} &\rightarrow \mathbb{C}^{n_1 \times n_2} \\ H &\mapsto F_{n_1}^{-1} H F_{n_2}^{-1}. \end{aligned} \quad (21)$$

Analogously to the 1D problem, we are interested in the function

$$\begin{aligned} \mathcal{F}_G : \mathbb{C}^{n_1 \times n_2} &\rightarrow \mathbb{C}^{n_1 \times n_2} \\ X &\mapsto \text{DFT}_{n_1 \times n_2}^{-1} (G \circ \text{DFT}_{n_1 \times n_2}(X)) \end{aligned} \quad (22)$$

for some  $G \in \mathbb{C}^{n_1 \times n_2}$ , where  $\circ$  is the Hadamard product. Once again, you can consider  $G = \text{DFT}_{n_1 \times n_2}(H)$  for some  $H \in \mathbb{C}^{n_1 \times n_2}$ , in which case  $\mathcal{F}_G(X)$  is the discrete convolution of  $X$  with  $H$  denoted by  $H * X$ . In matrix form, we have

$$\mathcal{F}_G(X) = F_{n_1}^{-1} (G \circ (F_{n_1} X F_{n_2})) F_{n_2}^{-1}. \quad (23)$$

As tempting as it may seem, we cannot distribute  $F_{n_2}^{-1}$  from the right as the Hadamard product is not distributive over matrix multiplication, i.e.,  $(G \circ X)Y \neq G \circ (XY)$ .

Let us now introduce vectorization, namely

$$\begin{aligned} \text{vec} : \mathbb{C}^{n_1 \times n_2} &\rightarrow \mathbb{C}^{n_1 n_2} \\ X &\mapsto \begin{bmatrix} X_{1:n_1,1} \\ X_{1:n_1,2} \\ \vdots \\ X_{1:n_1,n_2} \end{bmatrix}. \end{aligned} \quad (24)$$

Then, for all  $A \in \mathbb{C}^{n_1 \times n_1}$ ,  $X \in \mathbb{C}^{n_1 \times n_2}$  and  $B \in \mathbb{C}^{n_2 \times n_2}$ , we have

$$\text{vec}(AXB) = (B^T \otimes A) \cdot \text{vec}(X) \quad (25)$$

where  $\otimes$  denotes the Kronecker product so that, due to the symmetry of Fourier matrices, we have

$$\text{vec}(F_{n_1} X F_{n_2}) = (F_{n_2}^T \otimes F_{n_1}) \cdot \text{vec}(X) = (F_{n_2} \otimes F_{n_1}) \cdot \text{vec}(X) \quad (26)$$

and, similarly, for the inverse transforms:

$$\text{vec}(F_{n_1}^{-1} H F_{n_2}^{-1}) = (F_{n_2}^{-T} \otimes F_{n_1}^{-1}) \cdot \text{vec}(H) = (F_{n_2}^{-1} \otimes F_{n_1}^{-1}) \cdot \text{vec}(H). \quad (27)$$

Using Eq. (27) along with Eq. (23), we get

$$\text{vec}(\mathcal{F}_G(X)) = (F_{n_2}^{-1} \otimes F_{n_1}^{-1}) \cdot \text{vec}(G \circ (F_{n_1} X F_{n_2})) \quad (28)$$

in which using Eq. (26) leads to

$$\text{vec}(\mathcal{F}_G(X)) = (F_{n_2}^{-1} \otimes F_{n_1}^{-1}) \cdot \text{vec}(G \circ ((F_{n_2} \otimes F_{n_1}) \cdot \text{vec}(X))). \quad (29)$$

One can easily verify that

$$\text{vec}(G \circ ((F_{n_2} \otimes F_{n_1}) \cdot \text{vec}(X))) = \text{vec}(G) \circ ((F_{n_2} \otimes F_{n_1}) \cdot \text{vec}(X)) \quad (30)$$

so that Eq. (29) can be recast into

$$\text{vec}(\mathcal{F}_G(X)) = (F_{n_2}^{-1} \otimes F_{n_1}^{-1}) \cdot [\text{vec}(G) \circ ((F_{n_2} \otimes F_{n_1}) \cdot \text{vec}(X))] \quad (31)$$

which we can rewrite as

$$\text{vec}(\mathcal{F}_G(X)) = (F_{n_2}^{-1} \otimes F_{n_1}^{-1}) \cdot \text{diag}(\text{vec}(G)) \cdot (F_{n_2} \otimes F_{n_1}) \cdot \text{vec}(X). \quad (32)$$

### 3.1 Permutation-avoiding 2D convolution

Using  $F_n = P_{r,n} A_{r,n}^T$  along with the fact that  $(AB) \otimes (CD) = (A \otimes C) \cdot (B \otimes D)$ , we get

$$F_{n_2} \otimes F_{n_1} = (P_{r,n_2} A_{r,n_2}^T) \otimes (P_{r,n_1} A_{r,n_1}^T) = (P_{r,n_2} \otimes P_{r,n_1}) \cdot (A_{r,n_2}^T \otimes A_{r,n_1}^T). \quad (33)$$

Similarly, using  $F_n^{-1} = \overline{A_{r,n}} P_{r,n}/n$ , we get

$$F_{n_2}^{-1} \otimes F_{n_1}^{-1} = (\overline{A_{r,n_2}} P_{r,n_2}) \otimes (\overline{A_{r,n_1}} P_{r,n_1}) / (n_1 n_2) = (\overline{A_{r,n_2}} \otimes \overline{A_{r,n_1}}) \cdot (P_{r,n_2} \otimes P_{r,n_1}) / (n_1 n_2) \quad (34)$$

so that using Eqs. (33)-(34) into Eq. (32) leads to

$$\text{vec}(\mathcal{F}_G(X)) = \quad (35)$$

$$(\overline{A_{r,n_2}} \otimes \overline{A_{r,n_1}}) \cdot (P_{r,n_2} \otimes P_{r,n_1}) \cdot \text{diag}(\text{vec}(G)) \cdot (P_{r,n_2} \otimes P_{r,n_1}) \cdot (A_{r,n_2}^T \otimes A_{r,n_1}^T) \cdot \text{vec}(X) / (n_1 n_2).$$

Since  $P_{r,n_2} \otimes P_{r,n_1}$  is a symmetric permutation matrix, we have

$$(P_{r,n_2} \otimes P_{r,n_1}) \cdot \text{diag}(\text{vec}(G)) \cdot (P_{r,n_2} \otimes P_{r,n_1}) = \text{diag}((P_{r,n_2} \otimes P_{r,n_1}) \cdot \text{vec}(G)) \quad (36)$$

and Eq. (35) becomes

$$\text{vec}(\mathcal{F}_G(X)) = (\overline{A_{r,n_2}} \otimes \overline{A_{r,n_1}}) \cdot \text{diag}((P_{r,n_2} \otimes P_{r,n_1}) \cdot \text{vec}(G)) \cdot (A_{r,n_2}^T \otimes A_{r,n_1}^T) \cdot \text{vec}(X) / (n_1 n_2) \quad (37)$$

which we recast into

$$\text{vec}(\mathcal{F}_G(X)) = (\overline{A_{r,n_2}} \otimes \overline{A_{r,n_1}}) \cdot \text{diag}(\widehat{g}) \cdot (A_{r,n_2}^T \otimes A_{r,n_1}^T) \cdot \text{vec}(X) / (n_1 n_2) \quad (38)$$

or, equivalently,

$$\text{vec}(\mathcal{F}_G(X)) = (\overline{A_{r,n_2}} \otimes \overline{A_{r,n_1}}) \cdot (\widehat{g} \circ ((A_{r,n_2}^T \otimes A_{r,n_1}^T) \cdot \text{vec}(X))) / (n_1 n_2) \quad (39)$$

with

$$\widehat{g} := (P_{r,n_2} \otimes P_{r,n_1}) \cdot \text{vec}(G). \quad (40)$$

We have

$$\mathcal{F}_G(X) = \text{vec}^{-1} \left( (\overline{A_{r,n_2}} \otimes \overline{A_{r,n_1}}) \cdot (\widehat{g} \circ ((A_{r,n_2}^T \otimes A_{r,n_1}^T) \cdot \text{vec}(X))) \right) / (n_1 n_2). \quad (41)$$

In practice, we are concerned with the case in which we are equipped with a single given  $G \in \mathbb{C}^{n_1 \times n_2}$ , and we want to evaluate  $X \mapsto \mathcal{F}_G(X)$  for a sequence  $X_1, X_2, \dots \in \mathbb{C}^{n_1 \times n_2}$ . In that case, the permutation-avoiding convolution suggested by Eq. (41) requires a single offline application of the permutation matrix  $P_{r,n_2} \otimes P_{r,n_1}$  for the construction of  $\widehat{g}$ , whereas each online evaluation of  $\mathcal{F}_G$  is index-reversal-free. On the other hand, a naive application of Eqs. (22)-(23) requires *two applications of the permutation matrix*  $P_{r,n_2} \otimes P_{r,n_1}$  *for each evaluation of*  $\mathcal{F}_G$ .

## 4 Multi-dimensional problem

Consider the  $d$ -dimensional DFT applied to a  $d$ -way tensor  $\mathcal{X} \in \mathbb{C}^{n_1 \times \dots \times n_d}$ . The forward DFT is defined as

$$\text{DFT}_{n_1 \times \dots \times n_d} : \mathbb{C}^{n_1 \times \dots \times n_d} \rightarrow \mathbb{C}^{n_1 \times \dots \times n_d} \quad (42)$$

$$\mathcal{X} \mapsto \text{vec}^{-1}((F_{n_d} \otimes \dots \otimes F_{n_1}) \cdot \text{vec}(\mathcal{X}))$$

and its inverse is given by

$$\text{DFT}_{n_1 \times \dots \times n_d}^{-1} : \mathbb{C}^{n_1 \times \dots \times n_d} \rightarrow \mathbb{C}^{n_1 \times \dots \times n_d} \quad (43)$$

$$\mathcal{H} \mapsto \text{vec}^{-1}((F_{n_d}^{-1} \otimes \dots \otimes F_{n_1}^{-1}) \cdot \text{vec}(\mathcal{H}))$$

in which the invertible vectorization operator for a  $d$ -way tensor  $\mathcal{X} \in \mathbb{C}^{n_1 \times \dots \times n_d}$  is given by

$$\text{vec} : \mathbb{C}^{n_1 \times \dots \times n_d} \rightarrow \mathbb{C}^{n_1 \dots n_d} \quad (44)$$

$$\mathcal{X} \mapsto [\mathcal{X}_{1:n_1, 11 \dots 1}^T, \dots, \mathcal{X}_{1:n_1, n_2 1 \dots 1}^T, \mathcal{X}_{1:n_1, 12 \dots 1}^T, \dots, \mathcal{X}_{1:n_1, n_2 2 \dots 1}^T, \dots, \mathcal{X}_{n_1 n_2 \dots n_d}^T]^T.$$

That is, the entries of  $\mathcal{X}$  are stacked by increasing index in the last mode, then the second-to-last, and so on, with the first index varying fastest. Note that the  $\otimes$  operator in those definitions of the multi-dimensional DFT and its inverse is still a Kronecker product, not to be confused with a tensor product, i.e.,  $F_{n_d} \otimes \dots \otimes F_{n_1}$  is a  $n \times n$  matrix with  $n = n_1 \dots n_d$  also known as a 2-way tensor.

To perform a convolution of  $\mathcal{X} \in \mathbb{C}^{n_1 \times \dots \times n_d}$  with  $\mathcal{G} = \text{DFT}_{n_1 \times \dots \times n_d}(\mathcal{H})$  for some  $\mathcal{H} \in \mathbb{C}^{n_1 \times \dots \times n_d}$ , we define

$$\mathcal{F}_{\mathcal{G}} : \mathbb{C}^{n_1 \times \dots \times n_d} \rightarrow \mathbb{C}^{n_1 \times \dots \times n_d} \quad (45)$$

$$\mathcal{X} \mapsto \text{DFT}_{n_1 \times \dots \times n_d}^{-1}(\mathcal{G} \circ \text{DFT}_{n_1 \times \dots \times n_d}(\mathcal{X})).$$

Upon vectorizing  $\mathcal{X}$ , which stacks the tensor into a column vector, and using Kronecker product  $\otimes$  identities, we obtain:

$$\text{vec}(\mathcal{F}_{\mathcal{G}}(\mathcal{X})) = (F_{n_d}^{-1} \otimes \dots \otimes F_{n_1}^{-1}) \cdot \text{diag}(\text{vec}(\mathcal{G})) \cdot (F_{n_d} \otimes \dots \otimes F_{n_1}) \cdot \text{vec}(\mathcal{X}). \quad (46)$$

#### 4.1 Permutation-avoiding multi-dimensional convolution

To avoid index-reversal permutations at runtime, we factor each Fourier matrix as  $F_n = P_{r,n} A_{r,n}^T$  and its inverse as  $F_n^{-1} = \overline{A_{r,n}} P_{r,n} / n$ . We are then able to recast Eq. (46) as follows:

$$\text{vec}(\mathcal{F}_{\mathcal{G}}(\mathcal{X})) = (\overline{A_{r,n_d}} \otimes \dots \otimes \overline{A_{r,n_1}}) \cdot (\widehat{\mathcal{G}} \circ ((A_{r,n_d}^T \otimes \dots \otimes A_{r,n_1}^T) \cdot \text{vec}(\mathcal{X}))) / (n_1 \dots n_d) \quad (47)$$

where  $\widehat{\mathcal{G}}$  is computed offline as follows:

$$\widehat{\mathcal{G}} := (P_{r,n_d} \otimes \dots \otimes P_{r,n_1}) \cdot \text{vec}(\mathcal{G}). \quad (48)$$

Eventually, a convoluted  $d$ -way tensor can be recovered:

$$\mathcal{F}_{\mathcal{G}}(\mathcal{X}) = \text{vec}^{-1} \left( (\overline{A_{r,n_d}} \otimes \dots \otimes \overline{A_{r,n_1}}) \cdot (\widehat{\mathcal{G}} \circ ((A_{r,n_d}^T \otimes \dots \otimes A_{r,n_1}^T) \cdot \text{vec}(\mathcal{X}))) \right) / (n_1 \dots n_d). \quad (49)$$

This formulation allows the index-reversal permutation  $P_{r,n_d} \otimes \dots \otimes P_{r,n_1}$  to be applied only once during preprocessing of  $\mathcal{G}$ , which enables repeated applications of  $\mathcal{F}_{\mathcal{G}}$  to multiple inputs without incurring further permutation costs, whereas a standard FFT-based approach would require *two applications of the index-reversal permutation per evaluation of  $\mathcal{F}_{\mathcal{G}}$* .

## 5 Algorithms

Although our presentation of the Cooley-Tukey framework is matrix-based, its traditional implementation, and what we implemented in <https://github.com/venkovic/c-permutation-avoiding-convolution>, are not. Similarly, although the basic idea of Cooley-Tukey algorithms is recursive, most implementations, including ours, rearrange the algorithm to avoid explicit recursion and optimize memory access patterns. A more detailed description of the fundamental kernels used throughout this study is provided in Section A.

As is representative of common practice—our implementation included—the performance of FFT algorithms is evaluated assuming precomputation of twiddle factors. In general, a greater radix leads to smaller numbers of floating-point operations (FLOP). In particular, for Cooley-Tukey algorithms, we have:

- Radix-2:  $5 \log_2 n$  FLOP.
- Radix-4:  $4.25 \log_2 n$  FLOP.
- Radix-8:  $4.08 \log_2 n$  FLOP.

However, the number of FLOP only draws an incomplete picture of actual performance. In practice, memory access complexity also carries a significant effect on real-world performance. For a complete FFT evaluation, the memory access pattern consists of: (i) butterfly operations, which exhibit regular stride patterns with high spatial and temporal locality; (ii) index-reversal permutations, which create pseudo-random access patterns with poor cache behavior; and (iii) twiddle factor access, which is generally regular and cacheable when precomputed.

To better understand algorithm performance on modern processors, the roofline model provides a framework that relates arithmetic intensity to achievable performance. Arithmetic intensity, defined as the ratio of floating-point operations to memory traffic, determines whether an algorithm is compute-bound or memory-bound on a given architecture. While butterfly operations achieve high arithmetic intensity through the reuse of loaded data elements, permutations have zero arithmetic intensity—every memory access serves only to move data without computation.

The key insight is that index-reversal permutations, despite not involving any floating-point arithmetic, can consume a significant fraction of total execution time due to their memory-bound nature. For larger problem sizes that exceed cache capacity, our FFT kernels operate in memory-bound regimes where permutation costs become the dominant performance bottleneck. This memory-bound behavior explains why theoretical FLOP reductions from higher radices do not necessarily translate to performance improvements when permutation overhead overwhelms the computational savings.

The memory access behavior of index-reversal permutations exhibits scaling properties that become increasingly problematic with problem size. For a 1D problem of size  $n = r^t$ , the permutation requires  $n$  load operations and  $n$  store operations. However, the stride pattern depends on the radix structure:

- Radix-2: Access patterns alternate between stride-1 (sequential) and stride- $n/2$  operations.
- Radix-4: More complex patterns with strides of  $n/4$ ,  $n/2$ ,  $3n/4$ .
- General radix- $r$ :  $r$ -way interleaved access with strides of  $n/r$ ,  $2n/r$ ,  $\dots$ ,  $(r-1)n/r$ .

As  $n$  grows beyond cache capacity, these large strides force main memory access with significantly higher latency than cached operations. For modern processors with cache hierarchies, this creates a performance cliff where the permutation cost increases super-linearly with problem size once the working set exceeds the largest cache level.

Our implementation of the Cooley-Tukey FFT is meticulously decomposed into modular and transparent components: a precomputed index-reversal permutation, a precomputed twiddle factor array, and an efficient in-place, split-complex, and unordered FFT kernels. This deliberate separation allows us to not only evaluate the overall FFT cost but also to isolate and quantify the contribution of the index-reversal permutation step and the main butterfly computation independently. This modular approach provides several advantages. First, we can precisely measure the cost of permutations versus butterfly operations. Second, changes to permutation handling can be evaluated in isolation. Third, memory access costs can be studied independently of computational costs. Lastly, the impact of different cache hierarchies and memory systems can be assessed. Crucially, this structured approach mirrors the practical use-case modeled by FFTW when called with the `FFTW_ESTIMATE` flag: that is, a scenario where no architecture-specific optimizations (e.g., vectorization, cache-aware blocking, or fused twiddle application) are applied beyond basic algorithmic design.

The algorithms presented below represent different trade-offs between computational efficiency and memory access patterns, providing a foundation for understanding when permutation-avoiding strategies offer the greatest benefit.



- Algo. 1 (**Index-reversal permutation**) isolates the pure memory movement cost, providing a baseline for understanding the overhead that our permutation-avoiding approach eliminates.
- Algo. 2 (**Unordered forward FFT**) performs only butterfly operations without any permutations, achieving optimal arithmetic intensity but producing results in index-reversed order.
- Algo. 3 (**Forward FFT**) represents the standard approach, combining both permutation and butterfly costs.
- Algo. 4 (**Unordered backward FFT**) performs only conjugate butterfly operations without any permutations, achieving optimal arithmetic intensity but producing results in index-reversed order.
- Algo. 5 (**Backward FFT**) represents the standard approach, combining both permutation and conjugate butterfly costs.
- Algo. 6 (**Standard FFT-based convolution**) demonstrates the double permutation cost in traditional convolution implementations.
- Algo. 7 (**Permutation-avoiding convolution**) shows how our approach eliminates runtime permutations while maintaining correctness.

For small problems that fit entirely in cache, permutations may represent a small fraction of the total FFT runtime. However, as problem size grows beyond cache capacity, permutation costs should represent a greater part of the execution time due to their memory-bound nature, particularly for higher-dimensional problems where the memory access patterns become increasingly irregular. This scaling behavior creates a compelling case for permutation-avoiding approaches, especially in scenarios involving large problem sizes where cache effects become pronounced, multi-dimensional problems where access patterns are inherently irregular, and memory-constrained systems where bandwidth is the primary bottleneck.

---

**Algorithm 1** Index-reversal permutation

---

**Input:**  $\mathcal{X} \in \mathbb{C}^{n_1 \times \dots \times n_d}$ ,  $r$  s.t.  $\exists t_1, \dots, t_d$  s.t.  $n_1 = r^{t_1}, \dots, n_d = r^{t_d}$

- 1:  $x := (P_{r,n_d} \otimes \dots \otimes P_{r,n_1}) \cdot \text{vec}(\mathcal{X})$
  - 2: **return**  $\text{vec}^{-1}(x)$
- 

---

**Algorithm 2** Unordered forward FFT

---

**Input:**  $\mathcal{X} \in \mathbb{C}^{n_1 \times \dots \times n_d}$ ,  $r$  s.t.  $\exists t_1, \dots, t_d$  s.t.  $n_1 = r^{t_1}, \dots, n_d = r^{t_d}$

- 1:  $x := (A_{r,n_d} \otimes \dots \otimes A_{r,n_1}) \cdot \text{vec}(\mathcal{X})$
  - 2: **return**  $\text{vec}^{-1}(x)$
- 

---

**Algorithm 3** Forward FFT

---

**Input:**  $\mathcal{X} \in \mathbb{C}^{n_1 \times \dots \times n_d}$ ,  $r$  s.t.  $\exists t_1, \dots, t_d$  s.t.  $n_1 = r^{t_1}, \dots, n_d = r^{t_d}$

**Output:**  $\text{DFT}_{n_1 \times \dots \times n_d}(\mathcal{X}) \in \mathbb{C}^{n_1 \times \dots \times n_d}$

- 1:  $x := (P_{r,n_d} \otimes \dots \otimes P_{r,n_1}) \cdot \text{vec}(\mathcal{X})$
  - 2:  $x := (A_{r,n_d} \otimes \dots \otimes A_{r,n_1}) \cdot x$
  - 3: **return**  $\text{vec}^{-1}(x)$
- 

To characterize the performance regime of our algorithms within the roofline model framework, we assess theoretical estimates of arithmetic intensity. The FLOP count for FFT operations stems

**Algorithm 4** Unordered backward FFT**Input:**  $\mathcal{X} \in \mathbb{C}^{n_1 \times \dots \times n_d}$ ,  $r$  s.t.  $\exists t_1, \dots, t_d$  s.t.  $n_1 = r^{t_1}, \dots, n_d = r^{t_d}$ 

- 1:  $x := (\overline{A_{r,n_d}} \otimes \dots \otimes \overline{A_{r,n_1}}) \cdot \text{vec}(\mathcal{X})$
- 2: **return**  $\text{vec}^{-1}(x)/(n_1 \dots n_d)$

**Algorithm 5** Backward FFT**Input:**  $\mathcal{X} \in \mathbb{C}^{n_1 \times \dots \times n_d}$ ,  $r$  s.t.  $\exists t_1, \dots, t_d$  s.t.  $n_1 = r^{t_1}, \dots, n_d = r^{t_d}$ **Output:**  $\text{DFT}_{n_1 \times \dots \times n_d}^{-1}(\mathcal{X}) \in \mathbb{C}^{n_1 \times \dots \times n_d}$ 

- 1:  $x := (P_{r,n_d} \otimes \dots \otimes P_{r,n_1}) \cdot \text{vec}(\mathcal{X})$
- 2:  $x := (\overline{A_{r,n_d}} \otimes \dots \otimes \overline{A_{r,n_1}}) \cdot x$
- 3: **return**  $\text{vec}^{-1}(x)/(n_1 \dots n_d)$

**Algorithm 6** Standard FFT-based convolution**Input:**  $\mathcal{X} \in \mathbb{C}^{n_1 \times \dots \times n_d}$ ,  $r$  s.t.  $\exists t_1, \dots, t_d$  s.t.  $n_1 = r^{t_1}, \dots, n_d = r^{t_d}$ ,  $\mathcal{G} \in \mathbb{C}^{n_1 \times \dots \times n_d}$ **Output:**  $\text{DFT}_{n_1 \times \dots \times n_d}^{-1}(\mathcal{G} \circ \text{DFT}_{n_1 \times \dots \times n_d}(\mathcal{X})) \in \mathbb{C}^{n_1 \times \dots \times n_d}$ 

- 1:  $x := (P_{r,n_d} \otimes \dots \otimes P_{r,n_1}) \cdot \text{vec}(\mathcal{X})$
- 2:  $x := (\overline{A_{r,n_d}} \otimes \dots \otimes \overline{A_{r,n_1}}) \cdot x$
- 3:  $x := \text{vec}(\mathcal{G}) \circ x$
- 4:  $x := (P_{r,n_d} \otimes \dots \otimes P_{r,n_1}) \cdot x$
- 5:  $x := (\overline{A_{r,n_d}} \otimes \dots \otimes \overline{A_{r,n_1}}) \cdot x$
- 6: **return**  $\text{vec}^{-1}(x)/(n_1 \dots n_d)$

**Algorithm 7** Permutation-avoiding convolution — online phase**Input:**  $\mathcal{X} \in \mathbb{C}^{n_1 \times \dots \times n_d}$ ,  $r$  s.t.  $\exists t_1, \dots, t_d$  s.t.  $n_1 = r^{t_1}, \dots, n_d = r^{t_d}$ ,  $\mathcal{G} \in \mathbb{C}^{n_1 \times \dots \times n_d}$ **Output:**  $\text{DFT}_{n_1 \times \dots \times n_d}^{-1}(\mathcal{G} \circ \text{DFT}_{n_1 \times \dots \times n_d}(\mathcal{X})) \in \mathbb{C}^{n_1 \times \dots \times n_d}$ 

- 1:  $x := (A_{r,n_d}^T \otimes \dots \otimes A_{r,n_1}^T) \cdot \text{vec}(\mathcal{X})$
- 2:  $x := \widehat{g} \circ x$   $\triangleright \widehat{g} = (P_{r,n_d} \otimes \dots \otimes P_{r,n_1}) \cdot \text{vec}(\mathcal{G})$ , computed offline
- 3:  $x := (\overline{A_{r,n_d}} \otimes \dots \otimes \overline{A_{r,n_1}}) \cdot x$
- 4: **return**  $\text{vec}^{-1}(x)/(n_1 \dots n_d)$

entirely from butterfly operations, yielding  $5n \log_2 n$ ,  $4.25n \log_2 n$ , and  $4.08n \log_2 n$  FLOP for 1D radix-2, radix-4, and radix-8 implementations, respectively. While simplistic and incomplete, counting memory read and write accesses provides an initial estimate of memory traffic patterns. In 1D implementations, each of the  $\log_r n$  butterfly stages reads and writes  $n$  elements. The permutation operation contributes an additional  $n$  reads and  $n$  writes. This totals  $2n \cdot (1 + \log_r n)$  complex double-precision elements. For each FFT kernel, the theoretical arithmetic intensity becomes:

- Radix-2:  $(5n \log_2 n \text{ FLOP}) / (2n \cdot (1 + \log_2 n) \times 16 \text{ byte}) = 0.156(\log_2 n) / (1 + \log_2 n) \text{ FLOP/byte}$ ,
- Radix-4:  $(4.25n \log_2 n \text{ FLOP}) / (2n \cdot (1 + \log_4 n) \times 16 \text{ byte}) = 0.133(\log_2 n) / (1 + \log_4 n) \text{ FLOP/byte}$ ,
- Radix-8:  $(4.08n \log_2 n \text{ FLOP}) / (2n \cdot (1 + \log_8 n) \times 16 \text{ byte}) = 0.128(\log_2 n) / (1 + \log_8 n) \text{ FLOP/byte}$ .

These expressions indicate arithmetic intensity that increases with problem size  $n$  towards limits of 0.156, 0.266 and 0.383 FLOP/byte, respectively. Permutation-avoiding implementations reach these limits by reducing memory traffic to  $2n \log_r n$  accesses. Indeed, we have:

- Radix-2:  $(5n \log_2 n \text{ FLOP}) / (2n \log_2 n \times 16 \text{ byte}) = 0.156 \text{ FLOP/byte}$ ,

- Radix-4:  $(4.25n \log_2 n \text{ FLOP}) / (2n \log_4 n \times 16 \text{ byte}) = 0.266 \text{ FLOP/byte}$ ,
- Radix-8:  $(4.08n \log_2 n \text{ FLOP}) / (2n \log_8 n \times 16 \text{ byte}) = 0.383 \text{ FLOP/byte}$ .

Theoretically, permutation-avoiding implementations maintain constant arithmetic intensity independent of transform size. However, this analysis oversimplifies the memory hierarchy's complexity. In practice, data movement occurs across multiple memory levels, with performance determined by the algorithm's temporal and spatial locality characteristics and the underlying memory architecture. As transform size  $n$  increases, locality degrades and memory traffic intensifies when data exceeds the capacity of successive cache levels. Consequently, profiling DRAM traffic provides a more representative measure of actual data movement costs.

## 6 Numerical experiments

In our experiments, we benchmark and verify our implementations against FFTW using FFTW\_ESTIMATE preparation plans. Since FFTW under FFTW\_ESTIMATE uses generic Cooley-Tukey strategies without empirical performance tuning, our comparison is inherently fair. By benchmarking both the complete FFT pipeline and isolated operations (index-reversal permutation and butterfly computations), we obtain fine-grained insights that highlight how a clean, portable general radix implementation performs relative to FFTW's general-purpose performance without platform-specific optimizations.

All experiments are conducted on two distinct computing systems:

*Computing system #1.* Dell Inspiron 14 5420 laptop with the following specifications:

- Processor: Intel Core i7-1255U (12th Generation Alder Lake)
  - Architecture: x86\_64 hybrid (2 performance cores + 8 efficiency cores, 12 threads total)
  - Base/Boost frequency: 400 MHz - 4.7 GHz (P-cores), 3.5 GHz (E-cores)
  - Cache hierarchy: L1 928 KiB, L2 6.5 MiB, L3 12 MiB
  - Instruction sets: AVX, AVX2, SSE 4.2
- Memory:  $2 \times 32 \text{ GiB DDR4}$ , peak bandwidth measured at 14.93 GB/s per core.
- Software Environment:
  - Operating System: Ubuntu 24.04.2 LTS (Noble Numbat)
  - Kernel: Linux 6.11.0-26-generic
  - Compiler: GCC 13.3.0

The 12 MiB L3 cache accommodates moderate-sized FFT transforms entirely in cache, while AVX2 support enables vectorized operations that significantly impact optimized FFTW implementations.

*Computing system #2.* Dual-socket Intel Xeon server with the following specifications:

- Processor: Intel Xeon Platinum 8480+ (4th Generation Sapphire Rapids)
  - Architecture: x86\_64 dual-socket ( $2 \times 56$  cores, 224 threads total)
  - Base/Boost frequency: 800 MHz - 3.8 GHz
  - Cache hierarchy: L1 8.8 MiB, L2 224 MiB, L3 210 MiB
  - Instruction sets: AVX, AVX2, AVX-512F/DQ/BW/VL, AMX (Advanced Matrix Extensions)
- Memory: 503 GiB DDR5, peak bandwidth measured at 9.17 GB/s per core.
- Software Environment:
  - Operating System: Red Hat Enterprise Linux 9.5
  - Kernel: Linux 5.14.0-503.40.1.el9\_5.x86\_64
  - Compiler: GCC 11.5.0

The massive 210 MiB L3 cache can accommodate very large FFT transforms entirely in cache, while AVX-512 and AMX support enable highly vectorized operations with significant performance advantages for FFTW implementations over AVX2.

With these technical specifications in hand, one can assess machine balance for each system and compare these values with the theoretical arithmetic intensities presented in Section 5 to evaluate whether, in theory, a kernel is compute-bound or memory-bound. In particular, assuming single-thread performance without explicit vectorization or specific instruction set optimizations, computing system #1 achieves a peak performance of 4.7 GFLOP/s and a single-core peak memory bandwidth of 14.93 GB/s. This yields a machine balance of 0.315 FLOP/byte, which suggests that radix-2 and radix-4 implementations are memory-bound, both with and without permutations. However, permutation-avoiding kernels of radix-8 operate in the compute-bound regime, irrespective of  $n$ , whereas full-FFT radix-8 kernels become compute-bound for  $n \geq 8^5$ . For computing system #2, we observe a single-core peak performance of 3.8 GFLOP/s and a peak memory bandwidth of 9.17 GB/s per core, resulting in a machine balance of 0.414 FLOP/byte. Under these conditions, all kernel implementations are memory-bound.

### 6.1 1D results

Tables 1 and 2 present forward and backward FFT timing results on system #1, respectively. Runtimes measured on system #2 are presented in Tables 3 and 4. Several key observations emerge from these results:

Despite radix-8 requiring the fewest FLOP ( $4.08 \log_2 n$  vs  $4.25 \log_2 n$  for radix-4 and  $5 \log_2 n$  for radix-2), radix-4 consistently delivers the best performance across all problem sizes, on both systems. This counterintuitive result demonstrates that theoretical FLOP counts provide an incomplete picture of real-world performance.

The poor performance of radix-8 can be attributed to several factors: (i) scattered memory access patterns across 8 elements with large strides; (ii) increased register pressure from numerous temporary variables; and (iii) longer dependency chains that reduce instruction-level parallelism. These implementation overheads overwhelm the theoretical FLOP advantage.

For radix-4 implementations, index-reversal permutations account for 30–73% of total transform time, with the proportion increasing for larger problem sizes. This scaling occurs because permutations exhibit zero arithmetic intensity—pure memory movement without computation—while problem sizes exceed cache capacity.

Our radix-4 implementation achieves performance within  $1.5\times$  of FFTW across all problem sizes on system #1, and within  $2.2\times$  on system #2. The better performance of FFTW relative to our implementations on system #2 is likely due to AVX-512 and AMX support, while system #1 only allows for AVX2 instructions.

### 6.2 2D results

Tables 7, 8, 9 and 10 show 2D FFT results. The 2D case reveals important scaling behaviors:

Compared to 1D transforms of equivalent total size  $n = n_1 n_2$ , 2D permutations show significantly lower relative cost. This occurs because the Kronecker product structure  $P_{r,n_2} \otimes P_{r,n_1}$  creates access patterns where elements are permuted within neighborhoods of size  $n^{1/2}$ , improving spatial locality.

Conversely, 2D butterfly operations show higher per-element costs than their 1D counterparts, possibly due to the overhead of gathering and scattering column data, which requires additional memory copies and reduces effective cache utilization during the separable transform process.

Our implementations remain competitive with FFTW, often matching or slightly exceeding FFTW performance for larger problem sizes, particularly for radix-4.

### 6.3 3D results

Tables 13, 14, 15 and 16 present 3D FFT results, showing the continuation of trends observed in 2D:

Table 1. Timing of 1D index-reversal permutation, unordered and full forward FFT — Computing system #1

Procedure	$n = 2^{20}$	$n = 2^{22}$	$n = 2^{24}$	$n = 2^{26}$	$n = 2^{28}$
radix-2					
Index-reversal permutation	0.009 s	0.060 s	0.265 s	2.005 s	7.186 s
Unordered FFT	0.015 s	0.084 s	0.374 s	1.661 s	7.193 s
FFT	0.024 s	0.144 s	0.640 s	3.650 s	14.317 s
radix-4					
Index-reversal permutation	0.010 s	0.059 s	0.265 s	1.998 s	7.221 s
Unordered FFT	0.011 s	0.048 s	0.219 s	0.995 s	4.373 s
FFT	0.021 s	0.107 s	0.485 s	2.989 s	11.489 s
radix-8					
Index-reversal permutation	-	-	0.265 s	-	-
Unordered FFT	-	-	0.601 s	-	-
FFT	-	-	0.865 s	-	-
FFT (FFTW)	0.014 s	0.081 s	0.545 s	2.470 s	10.816 s

Table 2. Timing of 1D index-reversal permutation, unordered and full backward FFT — Computing system #1

Procedure	$n = 2^{20}$	$n = 2^{22}$	$n = 2^{24}$	$n = 2^{26}$	$n = 2^{28}$
radix-2					
Index-reversal permutation	0.009 s	0.059 s	0.262 s	2.019 s	7.101 s
Unordered FFT	0.016 s	0.089 s	0.387 s	1.726 s	7.493 s
FFT	0.025 s	0.151 s	0.647 s	3.790 s	14.612 s
radix-4					
Index-reversal permutation	0.009 s	0.057 s	0.261 s	2.003 s	7.181 s
Unordered FFT	0.011 s	0.059 s	0.255 s	1.071 s	4.736 s
FFT	0.020 s	0.117 s	0.513 s	3.009 s	12.214 s
radix-8					
Index-reversal permutation	-	-	0.261 s	-	-
Unordered FFT	-	-	0.622 s	-	-
FFT	-	-	0.877 s	-	-
FFT (FFTW)	0.015 s	0.089 s	0.559 s	2.559 s	11.389 s

The 3D case shows even lower relative permutation costs due to enhanced spatial locality from the three-dimensional Kronecker structure.

Multi-dimensional butterfly operations become increasingly expensive due to the complexity of managing three-dimensional memory access patterns.

Table 3. Timing of 1D index-reversal permutation, unordered and full forward FFT — Computing system #2

Procedure	$n = 2^{20}$	$n = 2^{22}$	$n = 2^{24}$	$n = 2^{26}$	$n = 2^{28}$
radix-2					
Index-reversal permutation	0.015 s	0.098 s	0.844 s	4.207 s	17.453 s
Unordered FFT	0.014 s	0.064 s	0.497 s	2.474 s	11.101 s
FFT	0.028 s	0.163 s	1.339 s	6.680 s	28.550 s
radix-4					
Index-reversal permutation	0.013 s	0.094 s	0.831 s	4.152 s	17.421 s
Unordered FFT	0.011 s	0.050 s	0.321 s	1.514 s	6.787 s
FFT	0.024 s	0.145 s	1.147 s	5.664 s	24.207 s
radix-8					
Index-reversal permutation	-	-	0.853 s	-	-
Unordered FFT	-	-	0.690 s	-	-
FFT	-	-	1.540 s	-	-
FFT (FFTW)	0.016 s	0.101 s	0.666 s	2.832 s	11.663 s

Table 4. Timing of 1D index-reversal permutation, unordered and full backward FFT — Computing system #2

Procedure	$n = 2^{20}$	$n = 2^{22}$	$n = 2^{24}$	$n = 2^{26}$	$n = 2^{28}$
radix-2					
Index-reversal permutation	0.017 s	0.088 s	0.843 s	4.176 s	17.240 s
Unordered FFT	0.014 s	0.066 s	0.516 s	2.546 s	11.258 s
FFT	0.031 s	0.155 s	1.361 s	6.721 s	28.497 s
radix-4					
Index-reversal permutation	0.014 s	0.086 s	0.832 s	4.137 s	17.194 s
Unordered FFT	0.011 s	0.052 s	0.339 s	1.612 s	7.114 s
FFT	0.026 s	0.138 s	1.171 s	5.747 s	24.309 s
radix-8					
Index-reversal permutation	-	-	0.854 s	-	-
Unordered FFT	-	-	0.715 s	-	-
FFT	-	-	1.562 s	-	-
FFT (FFTW)	0.016 s	0.101 s	0.698 s	2.889 s	11.822 s

## 6.4 Convolution results

Tables 5, 11, 17, 6, 12, and 18 demonstrate the effectiveness of our permutation-avoiding approach:

In 1D, permutation-avoiding convolution achieves up to  $3.2\times$  speedup over standard FFT-based convolution for radix-4, and up to  $3.6\times$  on system #2, with speedups generally increasing with problem size as permutation costs dominate.

Table 5. Timing of 1D permutation-avoiding and standard FFT-based convolution — Computing system #1

Procedure	$n = 2^{20}$	$n = 2^{22}$	$n = 2^{24}$	$n = 2^{26}$	$n = 2^{28}$
radix-2					
Permutation-avoiding convolution	0.031 s	0.181 s	0.775 s	4.325 s	18.793 s
Standard FFT-based convolution	0.047 s	0.315 s	1.346 s	8.444 s	33.355 s
radix-4					
Permutation-avoiding convolution	0.022 s	0.105 s	0.505 s	2.278 s	9.947 s
Standard FFT-based convolution	0.042 s	0.221 s	1.055 s	7.239 s	27.757 s
radix-8					
Permutation-avoiding convolution	-	-	1.280 s	-	-
Standard FFT-based convolution	-	-	1.855 s	-	-
Standard FFT-based convolution (FFTW)	0.030 s	0.199 s	1.145 s	5.098 s	21.172 s

Table 6. Timing of 1D permutation-avoiding and standard FFT-based convolution — Computing system #2

Procedure	$n = 2^{20}$	$n = 2^{22}$	$n = 2^{24}$	$n = 2^{26}$	$n = 2^{28}$
radix-2					
Permutation-avoiding convolution	0.031 s	0.166 s	1.171 s	5.621 s	25.205 s
Standard FFT-based convolution	0.063 s	0.331 s	2.745 s	13.507 s	57.705 s
radix-4					
Permutation-avoiding convolution	0.023 s	0.111 s	0.665 s	3.127 s	13.789 s
Standard FFT-based convolution	0.052 s	0.295 s	2.370 s	11.546 s	49.201 s
radix-8					
Permutation-avoiding convolution	-	-	1.403 s	-	-
Standard FFT-based convolution	-	-	3.149 s	-	-
Standard FFT-based convolution (FFTW)	0.033 s	0.214 s	1.336 s	5.716 s	23.880 s

Table 7. Timing of 2D index-reversal permutation, unordered and full forward FFT — Computing system #1

Procedure	$n_1 = n_2 = 2^{10}$	$n_1 = n_2 = 2^{11}$	$n_1 = n_2 = 2^{12}$	$n_1 = n_2 = 2^{13}$	$n_1 = n_2 = 2^{14}$
radix-2					
Index-reversal permutation	0.001 s	0.006 s	0.056 s	0.287 s	1.422 s
Unordered FFT	0.025 s	0.184 s	1.008 s	4.481 s	22.105 s
FFT	0.026 s	0.189 s	1.065 s	4.808 s	23.947 s
radix-4					
Index-reversal permutation	0.001 s	-	0.060 s	-	1.201 s
Unordered FFT	0.027 s	-	1.024 s	-	19.387 s
FFT	0.028 s	-	1.085 s	-	20.781 s
FFT (FFTW)	0.025 s	0.127 s	0.932 s	4.555 s	31.894 s

Table 8. Timing of 2D index-reversal permutation, unordered and full backward FFT — Computing system #1

Procedure	$n_1 = n_2 = 2^{10}$	$n_1 = n_2 = 2^{11}$	$n_1 = n_2 = 2^{12}$	$n_1 = n_2 = 2^{13}$	$n_1 = n_2 = 2^{14}$
radix-2					
Index-reversal permutation	0.001 s	0.006 s	0.057 s	0.293 s	1.297 s
Unordered FFT	0.023 s	0.189 s	1.014 s	4.579 s	19.829 s
FFT	0.024 s	0.192 s	1.070 s	4.887 s	20.951 s
radix-4					
Index-reversal permutation	0.001 s	-	0.061 s	-	1.326 s
Unordered FFT	0.024 s	-	1.038 s	-	20.592 s
FFT	0.025 s	-	1.099 s	-	21.716 s
FFT (FFTW)	0.022 s	0.159 s	0.887 s	4.830 s	25.869 s

Table 9. Timing of 2D index-reversal permutation, unordered and full forward FFT — Computing system #2

Procedure	$n_1 = n_2 = 2^{10}$	$n_1 = n_2 = 2^{11}$	$n_1 = n_2 = 2^{12}$	$n_1 = n_2 = 2^{13}$	$n_1 = n_2 = 2^{14}$
radix-2					
Index-reversal permutation	0.002 s	0.007 s	0.070 s	0.341 s	1.474 s
Unordered FFT	0.035 s	0.141 s	1.175 s	5.809 s	23.530 s
FFT	0.037 s	0.148 s	1.230 s	6.151 s	25.002 s
radix-4					
Index-reversal permutation	0.001 s	-	0.065 s	-	1.380 s
Unordered FFT	0.034 s	-	1.141 s	-	23.166 s
FFT	0.035 s	-	1.213 s	-	24.548 s
FFT (FFTW)	0.031 s	0.161 s	1.707 s	7.225 s	41.867 s



Table 10. Timing of 2D index-reversal permutation, unordered and full backward FFT — Computing system #2

Procedure	$n_1 = n_2 = 2^{10}$	$n_1 = n_2 = 2^{11}$	$n_1 = n_2 = 2^{12}$	$n_1 = n_2 = 2^{13}$	$n_1 = n_2 = 2^{14}$
radix-2					
Index-reversal permutation	0.002 s	0.007 s	0.070 s	0.340 s	1.473 s
Unordered FFT	0.036 s	0.143 s	1.146 s	5.849 s	24.035 s
FFT	0.038 s	0.150 s	1.214 s	6.189 s	25.504 s
radix-4					
Index-reversal permutation	0.002 s	-	0.065 s	-	1.403 s
Unordered FFT	0.034 s	-	1.128 s	-	24.024 s
FFT	0.036 s	-	1.190 s	-	25.413 s
FFT (FFTW)	0.032 s	0.162 s	1.668 s	7.209 s	42.074 s

Table 11. Timing of 2D permutation-avoiding and standard FFT-based convolution — Computing system #1

Procedure	$n_1 = n_2 = 2^{10}$	$n_1 = n_2 = 2^{11}$	$n_1 = n_2 = 2^{12}$	$n_1 = n_2 = 2^{13}$	$n_1 = n_2 = 2^{14}$
radix-2					
Permutation-avoiding convolution	0.052 s	0.368 s	2.046 s	9.684 s	41.535 s
Standard FFT-based convolution	0.051 s	0.388 s	2.194 s	10.290 s	44.392 s
radix-4					
Permutation-avoiding convolution	0.053 s	-	2.071 s	-	37.069 s
Standard FFT-based convolution	0.054 s	-	2.200 s	-	39.415 s
Standard FFT-based convolution (FFTW)	0.041 s	0.230 s	1.759 s	10.318 s	63.973 s

While absolute speedups decrease in higher dimensions due to reduced relative permutation costs, permutation-avoiding methods consistently outperform standard approaches, with improvements of 2–5% typical for 2D and 3D cases.

Our permutation-avoiding convolutions frequently outperform FFTW’s standard convolution implementation, particularly for larger 1D problems where permutation costs are most significant.

## 6.5 Scaling analysis

Figures 1 and 2 provide crucial insights into the scaling behavior of our algorithms:

Average per-element permutation costs increase with total size  $n$  but decrease dramatically with dimension  $d$  at fixed  $n$ . While the average per-element costs reported appear significantly smaller than typical runtime measurement precision, these values are obtained by dividing the total kernel runtime—itsself a meaningful and accurate measurement—by the transform size. The improvement

Table 12. Timing of 2D permutation-avoiding and standard FFT-based convolution — Computing system #2

Procedure	$n_1 = n_2 = 2^{10}$	$n_1 = n_2 = 2^{11}$	$n_1 = n_2 = 2^{12}$	$n_1 = n_2 = 2^{13}$	$n_1 = n_2 = 2^{14}$
radix-2					
Permutation-avoiding convolution	0.071 s	0.285s	2.236 s	11.859 s	48.105 s
Standard FFT-based convolution	0.075 s	0.305s	2.397 s	12.589 s	51.243 s
radix-4					
Permutation-avoiding convolution	0.064 s	-	2.202 s	-	47.562 s
Standard FFT-based convolution	0.070 s	-	2.326 s	-	50.636 s
Standard FFT-based convolution (FFTW)	0.064 s	0.381 s	3.324 s	14.567 s	85.845 s

Table 13. Timing of 3D index-reversal permutation, unordered and full forward FFT — Computing system #1

Procedure	$n_1 = n_2 = n_3 = 2^7$	$n_1 = n_2 = n_3 = 2^8$	$n_1 = n_2 = n_3 = 2^9$
radix-2			
Index-reversal permutation	0.003 s	0.023 s	0.189 s
Unordered FFT	0.106 s	1.103 s	9.562 s
FFT	0.108 s	1.124 s	9.667 s
radix-4			
Index-reversal permutation	-	0.023 s	-
Unordered FFT	-	1.129 s	-
FFT	-	1.160 s	-
FFT (FFTW)	0.018 s	1.147 s	7.354 s

from 1D to 2D and from 2D to 3D each provides nearly an order of magnitude reduction, directly attributable to enhanced spatial locality arising from the Kronecker product structure.

Per-element butterfly costs show the inverse trend, increasing with both total size  $n$  and dimension  $d$ . This reflects the increasing complexity of multi-dimensional memory access patterns required for separable transforms.

These opposing trends suggest that permutation-avoiding techniques provide the greatest benefits for: (i) large 1D problems where permutation costs dominate; (ii) multi-dimensional problems with large sizes in one dimension; and (iii) systems with sufficiently small cache.

The experimental results demonstrate that while theoretical FLOP counts provide useful guidance, real-world FFT performance requires careful consideration of memory hierarchy effects, instruction-level parallelism, and the arithmetic intensity of different algorithmic components. Our permutation-avoiding approach successfully exploits this understanding to achieve meaningful performance improvements in practically relevant scenarios.

Table 14. Timing of 3D index-reversal permutation, unordered and full backward FFT — Computing system #1

Procedure	$n_1 = n_2 = n_3 = 2^7$	$n_1 = n_2 = n_3 = 2^8$	$n_1 = n_2 = n_3 = 2^9$
radix-2			
Index-reversal permutation	0.002 s	0.022 s	0.193 s
Unordered FFT	0.062 s	1.190 s	8.457 s
FFT	0.064 s	1.213 s	8.624 s
radix-4			
Index-reversal permutation	-	0.022 s	-
Unordered FFT	-	1.212 s	-
FFT	-	1.247 s	-
FFT (FFTW)	0.021 s	1.180 s	11.057 s

Table 15. Timing of 3D index-reversal permutation, unordered and full forward FFT — Computing system #2

Procedure	$n_1 = n_2 = n_3 = 2^7$	$n_1 = n_2 = n_3 = 2^8$	$n_1 = n_2 = n_3 = 2^9$
radix-2			
Index-reversal permutation	0.002 s	0.028 s	0.270 s
Unordered FFT	0.079 s	0.807 s	10.136 s
FFT	0.081 s	0.836 s	10.414 s
radix-4			
Index-reversal permutation	-	0.029 s	-
Unordered FFT	-	0.768 s	-
FFT	-	0.799 s	-
FFT (FFTW)	0.014 s	0.977 s	10.913 s

## 7 Discussion

In this section, we investigate the applicability of our permutation-avoiding convolution procedure to other FFT frameworks, namely the mixed-radix case, the prime factor framework, Rader's and Bluestein's algorithms as well as the four-step method.

### 7.1 Mixed-radix framework

Although we aimed to keep our treatment of the Cooley-Tukey framework as general as possible (see Section 2.1), we still assumed that each recursion step subdivides the problem into  $r$  equal-sized subproblems. That is, we used a uniform radix. In practice, a more general and widely used approach is the mixed-radix framework, in which  $n$  is factored into a product of  $t$  integers, i.e.,  $n = r_1 \cdots r_t$ .

The resulting Fourier matrix retains its fundamental properties, as these are independent of the framework adopted. However, the factorization itself differs. Within the Cooley-Tukey framework,

Table 16. Timing of 3D index-reversal permutation, unordered and full backward FFT — Computing system #2

Procedure	$n_1 = n_2 = n_3 = 2^7$	$n_1 = n_2 = n_3 = 2^8$	$n_1 = n_2 = n_3 = 2^9$
radix-2			
Index-reversal permutation	0.002 s	0.028 s	0.270 s
Unordered FFT	0.080 s	0.828 s	10.039 s
FFT	0.082 s	0.857 s	10.308 s
radix-4			
Index-reversal permutation	-	0.030 s	-
Unordered FFT	-	0.789 s	-
FFT	-	0.819 s	-
FFT (FFTW)	0.015 s	0.990 s	11.099 s

Table 17. Timing of 3D permutation-avoiding and standard FFT-based convolution — Computing system #1

Procedure	$n_1 = n_2 = n_3 = 2^7$	$n_1 = n_2 = n_3 = 2^8$	$n_1 = n_2 = n_3 = 2^9$
radix-2			
Permutation-avoiding convolution	0.193 s	2.318 s	16.176 s
Standard FFT-based convolution	0.198 s	2.380 s	16.607 s
radix-4			
Permutation-avoiding convolution	-	2.347 s	-
Standard FFT-based convolution	-	2.392 s	-
Standard FFT-based convolution (FFTW)	0.040 s	2.679 s	16.291 s

the mixed-radix approach leads to a decomposition of the form

$$F_n = A_{\rho,n} P_{\rho,n}^T, \quad (50)$$

where  $\rho := [r_1, \dots, r_t]$ . Here,  $A_{\rho,n} \in \mathbb{C}^{n \times n}$  is still a product of block butterfly matrices, while  $P_{\rho,n}$  is a permutation matrix, generally not symmetric, unlike the case in the uniform radix framework discussed in Section 2.1.

The matrix  $A_{\rho,n}$  has the form:

$$A_{\rho,n} = B_{r_t,n}(I_{n/(r_1 \cdots r_{t-1})} \otimes B_{r_{t-1},r_1 \cdots r_{t-1}}) \cdots (I_{n/(r_1 r_2)} \otimes B_{r_2,r_1 r_2})(I_{n/r_1} \otimes B_{r_1,r_1}), \quad (51)$$

where  $B_{r,n}$  is defined as in Eq. (8).

Similarly, the permutation matrix is given by:

$$P_{\rho,n} = \Pi_{r_t,n}(I_{n/(r_1 \cdots r_{t-1})} \otimes \Pi_{r_{t-1},r_1 \cdots r_{t-1}}) \cdots (I_{n/(r_1 r_2)} \otimes \Pi_{r_2,r_1 r_2})(I_{n/r_1} \otimes \Pi_{r_1,r_1}), \quad (52)$$

Table 18. Timing of 3D permutation-avoiding and standard FFT-based convolution — Computing system #2

Procedure	$n_1 = n_2 = n_3 = 2^7$	$n_1 = n_2 = n_3 = 2^8$	$n_1 = n_2 = n_3 = 2^9$
radix-2			
Permutation-avoiding convolution	0.161 s	1.664 s	21.163 s
Standard FFT-based convolution	0.167 s	1.734 s	21.718 s
radix-4			
Permutation-avoiding convolution	-	1.592 s	-
Standard FFT-based convolution	-	1.653 s	-
Standard FFT-based convolution (FFTW)	0.032 s	1.988 s	22.955 s

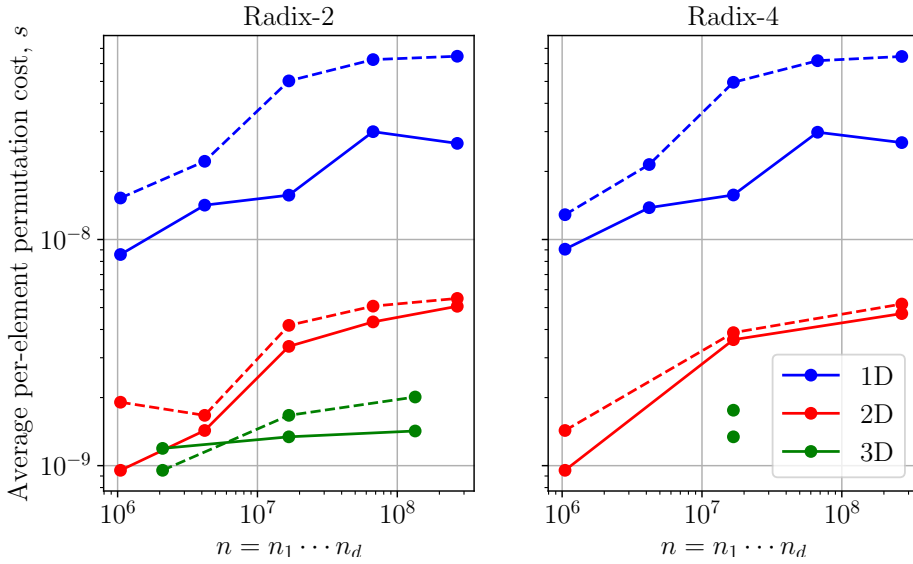


Fig. 1. Average per-element permutation cost for computing systems #1 (solid lines) and #2 (dashed lines)

where  $\Pi_{r,n}$  denotes a modulo- $r$  perfect shuffle permutation matrix, that is, the inverse of a modulo- $r$  sort permutation matrix. Note that both coincide when  $n$  is a power of  $r$ , as assumed in Section 2.1.

The transpose symmetry of the Fourier matrix still holds:

$$F_n = F_n^T = (A_{\rho,n} P_{\rho,n}^T)^T = P_{\rho,n} A_{\rho,n}^T. \quad (53)$$

Moreover, the inverse Fourier matrix satisfies:

$$F_n^{-1} = \overline{F_n}/n = \overline{A_{\rho,n} P_{\rho,n}^T} = \overline{A_{\rho,n}} P_{\rho,n}^T. \quad (54)$$

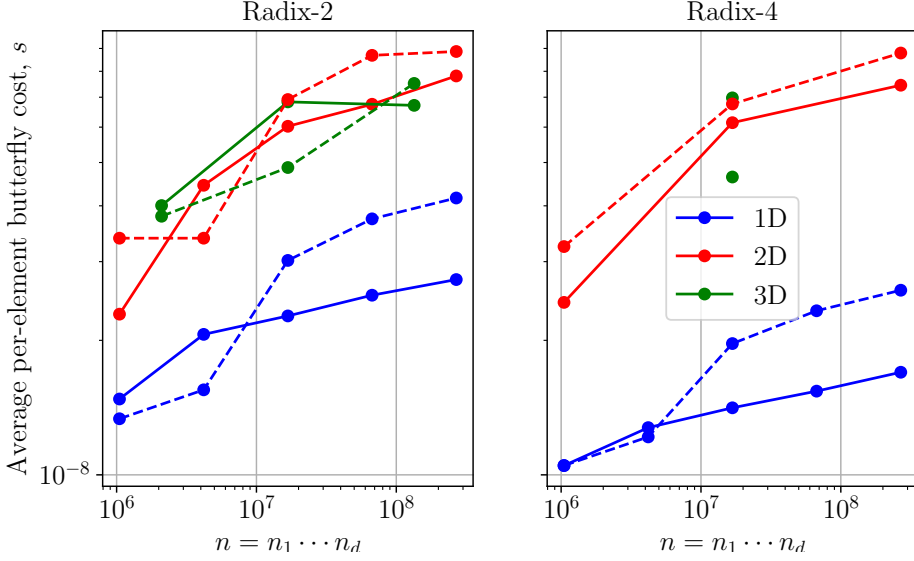


Fig. 2. Average per-element butterfly cost for computing systems #1 (solid lines) and #2 (dashed lines)

Putting all components together in the operator  $\mathcal{F}_g$ , we obtain:

$$\begin{aligned}
 \mathcal{F}_g(x) &= F_n^{-1} \text{diag}(g) F_n x \\
 &= \overline{A_{\rho,n}} P_{\rho,n}^T \text{diag}(g) P_{\rho,n} A_{\rho,n}^T / n \\
 &= \overline{A_{\rho,n}} \text{diag}(\widehat{g}) A_{\rho,n}^T / n \\
 &= \overline{A_{\rho,n}} (\widehat{g} \circ (A_{\rho,n}^T x)) / n,
 \end{aligned} \tag{55}$$

where

$$\widehat{g} := P_{\rho,n}^T g. \tag{56}$$

Consequently, the permutation-avoiding expression for  $\mathcal{F}_g$  given in Eq. (19) remains valid in the mixed-radix setting. However, the filter  $g$  must be permuted via  $P_{\rho,n}^T$ , which coincides with  $P_{\rho,n}$  in the uniform radix case.

Finally, all results in this subsection generalize directly to multi-dimensional mixed-radix FFTs. Hence, Algo. 7 remains valid, with only a minor adjustment required in the offline filter permutation.

## 7.2 Prime factor framework

Prime factor FFTs [Good 1958; Thomas 1963] rely on a number-theoretic decomposition of the Fourier matrix. Suppose  $n = n_1 \cdots n_t$  with  $n_1, \dots, n_t$  pairwise coprime. Then, there exist permutation matrices  $\Gamma_\rho, \Upsilon_\rho \in \mathbb{R}^{n \times n}$  such that

$$F_n = \Gamma_\rho (F_{n_t} \otimes \cdots \otimes F_{n_1}) \Upsilon_\rho^T. \tag{57}$$

Assume now that each Fourier matrix  $F_{n_q}$  can be locally factored as  $F_{n_q} = A_{n_q} P_{n_q}^T$  for  $q = 1, \dots, t$ , with  $A_{n_q} \in \mathbb{C}^{n_q \times n_q}$  and  $P_{n_q} \in \mathbb{R}^{n_q \times n_q}$ . Then, we have

$$\begin{aligned}
 F_n &= F_n^T \\
 &= \left( \Gamma_\rho(F_{n_t} \otimes \dots \otimes F_{n_1}) \Upsilon_\rho^T \right)^T \\
 &= \left( \Gamma_\rho(A_{n_t} P_{n_t}^T) \otimes \dots \otimes (A_{n_1} P_{n_1}^T) \Upsilon_\rho^T \right)^T \\
 &= \Upsilon_\rho(P_{n_t} \otimes \dots \otimes P_{n_1}) (A_{n_t}^T \otimes \dots \otimes A_{n_1}^T) \Gamma_\rho^T
 \end{aligned} \tag{58}$$

and, similarly for the inverse Fourier matrix:

$$\begin{aligned}
 F_n^{-1} &= \overline{F_n}/n \\
 &= \overline{\Gamma_\rho(F_{n_t} \otimes \dots \otimes F_{n_1}) \Upsilon_\rho^T} / n \\
 &= \overline{\Gamma_\rho(A_{n_t} P_{n_t}^T) \otimes \dots \otimes (A_{n_1} P_{n_1}^T) \Upsilon_\rho^T} / n \\
 &= \Gamma_\rho(\overline{A_{n_t}} \otimes \dots \otimes \overline{A_{n_1}}) (P_{n_t}^T \otimes \dots \otimes P_{n_1}^T) \Upsilon_\rho^T / n
 \end{aligned} \tag{59}$$

so that the convolution  $\mathcal{F}_g(x) = F_n^{-1} \text{diag}(g) F_n x$  becomes

$$\mathcal{F}_g(x) = \Gamma_\rho(\overline{A_{n_t}} \otimes \dots \otimes \overline{A_{n_1}}) (\widehat{g} \circ ((A_{n_t}^T \otimes \dots \otimes A_{n_1}^T) \Gamma_\rho^T x)) / n, \tag{60}$$

where the permuted transformed filter is defined as

$$\widehat{g} := (P_{n_t}^T \otimes \dots \otimes P_{n_1}^T) \Upsilon_\rho^T g. \tag{61}$$

This formulation demonstrates that, upon introducing an offline filter permutation, the prime factor FFT-based convolution can be performed using only two permutations— $\Gamma_\rho^T$  before and  $\Gamma_\rho$  after the core computation—instead of four, thus enabling permutation-avoiding acceleration. Note that these observations generalize directly to multi-dimensional prime factor FFTs.

### 7.3 Rader's and Bluestein's frameworks

Both Rader's FFT [Rader 1968] and the Bluestein algorithm [Bluestein 1970] reformulate the discrete Fourier transform (DFT) as a convolution, which can then be efficiently computed using any suitable FFT framework. If the chosen FFT framework supports permutation-avoiding techniques, as demonstrated earlier, then Rader's and Bluestein's methods can also benefit from these optimizations.

### 7.4 Four-step framework

One of the most performant FFT frameworks is a blocking strategy initially proposed in [Gentleman and Sande 1966]. After being revisited in [Bailey 1990], it became known as the four-step FFT, and is sometimes even referred to as Bailey's algorithm.

The starting point of the four-step FFT is the radix- $r$  splitting. That is, suppose  $n = rm$ , then we have

$$F_n = (F_r \otimes I_m) \text{diag}(I_m, \Omega_{r,m}, \dots, \Omega_{r,m}^{r-1}) (I_r \otimes F_m) \Pi_{r,n}^T. \tag{62}$$

Let  $x \in \mathbb{C}^n$ , and denote by  $x_{m \times r}$  its  $m \times r$  column-major matrixification. Then, for any  $A \in \mathbb{C}^{r \times r}$ , we have  $((A \otimes I_m)x)_{m \times r} = x_{m \times r} A^T$ . Applying this identity yields

$$\begin{aligned} (F_n x)_{m \times r} &= ((F_r \otimes I_m) \text{diag}(I_m, \Omega_{r,m}, \dots, \Omega_{r,m}^{r-1})(I_r \otimes F_m) \Pi_{r,n}^T x)_{m \times r} \\ &= (\text{diag}(I_m, \Omega_{r,m}, \dots, \Omega_{r,m}^{r-1})(I_r \otimes F_m) \Pi_{r,n}^T x)_{m \times r} F_r \\ &= \left( (F_n)_{1:m,1:r} \circ ((I_r \otimes F_m) \Pi_{r,n}^T x)_{m \times r} \right) F_r. \end{aligned} \quad (63)$$

Using the additional Kronecker identity  $((I_r \otimes A)x)_{m \times r} = Ax_{m \times r}$  for  $A \in \mathbb{C}^{m \times m}$ , we obtain

$$(F_n x)_{m \times r} = \left( (F_n)_{1:m,1:r} \circ (F_m (\Pi_{r,n}^T x)_{m \times r}) \right) F_r. \quad (64)$$

Since  $\Pi_{r,n}^T$  is a modulo- $r$  sort permutation matrix, we have  $(\Pi_{r,n}^T x)_{m \times r} = x_{r \times m}^T$ , leading to

$$(F_n x)_{m \times r} = \left( (F_n)_{1:m,1:r} \circ (F_m x_{r \times m}^T) \right) F_r. \quad (65)$$

This is the final form of the four-step FFT. Note that the single-vector DFT  $F_n x$  is transformed into a sequence of DFTs on multiple vectors.

If the constituent DFTs are implemented via a radix-2 Cooley-Tukey algorithm, the total number of FLOP required by Eq. (65) is  $5n \log_2 n$ , which matches the complexity of the radix-2 Cooley-Tukey FFT. However, while the four-step framework does not reduce the overall FLOP count, its blocking strategy dramatically improves data locality and reuse, leading to some of the fastest known implementations.

Applying the four-step approach to the inverse DFT yields

$$(F_n^{-1} h)_{r \times m} = (\overline{F_n h})_{r \times m} / n \quad (66)$$

$$= \left( \overline{(F_n)_{1:r,1:m} \circ (\overline{F_r h_{m \times r}^T})} \right) \overline{F_m} / n \quad (67)$$

$$= n \left( \overline{(F_n)_{1:r,1:m} \circ (F_r^{-1} h_{m \times r}^T)} \right) F_m^{-1}. \quad (68)$$

Therefore, the convolution  $\mathcal{F}_g(x) = F_n^{-1}(g \circ (F_n x))$  can be written as

$$\begin{aligned} (\mathcal{F}_g(x))_{r \times m} &= n \left( \overline{(F_n^{-1})_{1:r,1:m} \circ \left( F_r^{-1}(g \circ (F_n x)_{m \times r}^T) \right)} \right) F_m^{-1} \\ &= n \left( \overline{(F_n^{-1})_{1:r,1:m} \circ \left( F_r^{-1} \left( g \circ \left( ((F_n)_{1:m,1:r} \circ (F_m x_{r \times m}^T)) F_r \right)^T \right) \right)} \right) F_m^{-1}. \end{aligned} \quad (69)$$

This results in a nine-step procedure consisting of multi-vector transforms, twiddle-factor scalings, and matrix transpositions:

- (1)  $x_{m \times r} := x_{r \times m}^T$
- (2)  $x_{m \times r} := F_m x_{m \times r}$
- (3)  $x_{m \times r} := (F_n)_{1:m,1:r} \circ x_{m \times r}$
- (4)  $x_{m \times r} := x_{m \times r} F_r$
- (5)  $x_{r \times m} := x_{m \times r}^T$
- (6)  $x_{r \times m} := g_{r \times m} \circ x_{r \times m}$
- (7)  $x_{r \times m} := \overline{F_r^{-1} x_{r \times m}}$
- (8)  $x_{r \times m} := (F_n^{-1})_{1:r,1:m} \circ x_{r \times m}$
- (9)  $x_{r \times m} := x_{r \times m} F_m^{-1}$

Upon detailed examination of the four-step framework and its application to discrete convolution, we conclude that it is unfortunately not amenable to permutation-avoiding techniques.



## 8 Conclusion

This work presents a comprehensive analysis of permutation-avoiding convolution algorithms within the general radix Cooley-Tukey framework, extending from one-dimensional to multi-dimensional transforms. Our key contributions demonstrate both theoretical insights and practical performance improvements for a common but previously underoptimized computational pattern.

Our theoretical analysis reveals that index-reversal permutations while representing zero arithmetic intensity, can dominate FFT execution time due to their memory-bound nature and poor cache behavior. By reformulating the mathematical structure of FFT-based convolution, we show that these permutations can be eliminated from the online computation phase through a single offline filter preprocessing step. This transformation reduces the permutation overhead from two applications per convolution to a single offline operation, regardless of the number of repeated evaluations.

The experimental validation across multiple radices (2, 4, and 8) and dimensions (1D, 2D, and 3D) provides several important insights. First, theoretical FLOP counts alone provide insufficient guidance for real-world performance optimization—our radix-4 implementation consistently outperformed radix-8 despite the latter’s 20% FLOP advantage, highlighting the critical importance of memory access patterns and register utilization. Second, the effectiveness of permutation-avoiding techniques exhibits strong dimensional dependence: 1D problems show dramatic speedups (up to 3.3X for large transforms), while multi-dimensional cases demonstrate more modest but consistent improvements due to improved spatial locality in higher-dimensional Kronecker products.

Our scaling analysis reveals the fundamental trade-off between permutation and butterfly costs across dimensions. While per-element permutation costs decrease dramatically with dimension due to enhanced spatial locality, butterfly operations become increasingly expensive due to non-contiguous memory access patterns. This analysis provides clear guidance for when permutation-avoiding approaches offer maximum benefit: large 1D problems where permutation costs dominate, multi-dimensional problems with large sizes in one dimension, and systems with sufficiently small cache.

The practical impact extends beyond our specific implementation. We demonstrate that the permutation-avoiding approach generalizes to mixed-radix, prime factor, and other Cooley-Tukey variants, making it applicable to production FFT libraries. Our modular implementation architecture, which cleanly separates permutation and butterfly operations, enables precise performance analysis and could inform the design of next-generation FFT libraries.

Several directions for future work emerge from this analysis. First, the integration of permutation-avoiding techniques with advanced optimization strategies such as cache blocking, vectorization, and multi-threading remains unexplored. In particular, our multi-dimensional implementations could benefit significantly from blocking strategies that process multiple rows or columns simultaneously, improving cache locality and reducing the gather-scatter overhead that currently limits 2D and 3D performance. Second, the extension to mixed-radix and other FFT frameworks could broaden applicability. Third, the potential for hardware-specific optimizations, particularly for architectures with different cache hierarchies or specialized memory access patterns, warrants investigation.

Our results suggest that developers of high-performance FFT libraries should consider supporting permutation-avoiding convolution kernels, particularly for applications involving repeated convolutions with fixed filters. The consistent performance improvements demonstrated across different problem sizes and dimensions, combined with the broad applicability to existing FFT frameworks, make this a compelling addition to the computational toolkit for signal processing, scientific computing, and machine learning applications.

This work reinforces the importance of considering memory hierarchy effects alongside computational complexity in algorithm design. As the gap between processor and memory performance continues to widen, techniques that minimize memory movement while preserving computational correctness become increasingly valuable for achieving optimal performance in numerical computing.

## References

- David H Bailey. 1990. FFTs in external or hierarchical memory. *The journal of Supercomputing* 4 (1990), 23–35.
- Leo Bluestein. 1970. A linear filtering approach to the computation of discrete Fourier transform. *IEEE Transactions on Audio and Electroacoustics* 18, 4 (1970), 451–455.
- Grace Chan and Andrew TA Wood. 1997. Algorithm AS 312: An Algorithm for simulating stationary Gaussian random fields. *Applied Statistics* (1997), 171–181.
- James W Cooley and John W Tukey. 1965. An algorithm for the machine calculation of complex Fourier series. *Mathematics of computation* 19, 90 (1965), 297–301.
- Colin R Dietrich and Garry N Newsam. 1993. A fast and exact method for multidimensional Gaussian stochastic simulations. *Water Resources Research* 29, 8 (1993), 2861–2869.
- Claude R Dietrich and Garry N Newsam. 1997. Fast and exact simulation of stationary Gaussian processes through circulant embedding of the covariance matrix. *SIAM Journal on Scientific Computing* 18, 4 (1997), 1088–1107.
- Pierre Duhamel and Henk Hollmann. 1984. ‘Split radix’ FFT algorithm. *Electronics letters* 20, 1 (1984), 14–16.
- Matteo Frigo and Steven G Johnson. 1998. FFTW: An adaptive software architecture for the FFT. In *Proceedings of the 1998 IEEE International Conference on Acoustics, Speech and Signal Processing, ICASSP’98 (Cat. No. 98CH36181)*, Vol. 3. IEEE, 1381–1384.
- Matteo Frigo and Steven G Johnson. 2005. The design and implementation of FFTW3. *Proc. IEEE* 93, 2 (2005), 216–231.
- W Morven Gentleman and Gordon Sande. 1966. Fast fourier transforms: for fun and profit. In *Proceedings of the November 7-10, 1966, fall joint computer conference*. 563–578.
- Rafael C Gonzalez. 2009. *Digital image processing*. Pearson Education India.
- Irving John Good. 1958. The interaction algorithm and practical Fourier analysis. *Journal of the Royal Statistical Society Series B: Statistical Methodology* 20, 2 (1958), 361–372.
- Intel Corporation. 2025. *Intel® Math Kernel Library Developer Reference*. <https://www.intel.com/content/www/us/en/developer/tools/oneapi/onemkl-documentation.html>.
- Hervé Moulinec and Pierre Suquet. 1998. A numerical method for computing the overall response of nonlinear composites with complex microstructure. *Computer methods in applied mechanics and engineering* 157, 1-2 (1998), 69–94.
- Alan V Oppenheim. 1999. *Discrete-time signal processing*. Pearson Education India.
- Charles M Rader. 1968. Discrete Fourier transforms when the number of data samples is prime. *Proc. IEEE* 56, 6 (1968), 1107–1108.
- Paul N Swarztrauber. 1977. The methods of cyclic reduction, Fourier analysis and the FACR algorithm for the discrete solution of Poisson’s equation on a rectangle. *SIAM Rev.* 19, 3 (1977), 490–501.
- Llewellyn H Thomas. 1963. Using a computer to solve problems in physics. *Applications of digital computers* (1963), 44–45.
- Charles Van Loan. 1992. *Computational frameworks for the fast Fourier transform*. SIAM.
- Andrew TA Wood and Grace Chan. 1994. Simulation of stationary Gaussian processes in  $[0, 1]^d$ . *Journal of computational and graphical statistics* 3, 4 (1994), 409–432.
- R Yavne. 1968. An economical method for calculating the discrete Fourier transform. *AFIPS ’68 (Fall, part I): Proceedings of the December 9-11, 1968, fall joint computer conference, part I* (1968), 115–125.
- Jan Zeman, Jaroslav Vondřejc, Jan Novák, and Ivo Marek. 2010. Accelerating a FFT-based solver for numerical homogenization of periodic media by conjugate gradients. *J. Comput. Phys.* 229, 21 (2010), 8065–8071.

## A FFT and convolution sub-kernel algorithms

In the algorithms presented in Section 5, for any given  $x \in \mathbb{C}^n$ , we need to evaluate  $A_{r,n}x$ ,  $\overline{A_{r,n}x}$  and  $A_{r,n}^T x$ . Irrespective of the radix, these kernels are implemented as described in Algos. 8 and 9. In what follows, we show detailed implementations of these kernels for radices 2, 4, and 8.

**Algorithm 8** Butterfly-related kernels**Input:**  $x \in \mathbb{C}^n$ **Output:**  $x := A_{r,n}x$  or  $x := \overline{A_{r,n}x}$ 

```

1: for  $q = 1, \dots, t$  do
2:    $k := r^q$ 
3:    $n_b := n/k$ 
4:   for  $b = 1, \dots, n_b$  do
5:      $x_{(b-1)k+1:bk} := B_{r,k}x_{(b-1)k+1:bk}$ 
6:     or  $x_{(b-1)k+1:bk} := \overline{B_{r,k}x_{(b-1)k+1:bk}}$ 
7:   end for
8: end for
9: return  $x$ 

```

**Algorithm 9** Transposed butterfly kernels**Input:**  $x \in \mathbb{C}^n$ **Output:**  $x := A_{r,n}^T x$ 

```

1: for  $q = t, \dots, 1$  do
2:    $k := r^q$ 
3:    $n_b := n/k$ 
4:   for  $b = 1, \dots, n_b$  do
5:      $x_{(b-1)k+1:bk} := B_{r,k}^T x_{(b-1)k+1:bk}$ 
6:   end for
7: end for
8: return  $x$ 

```

**A.1 Radix-2 butterfly-related kernels**

For the radix-2 case, we have

$$B_{2,k} = (F_2 \otimes I_{k/2}) \text{diag}(I_{k/2}, \Omega_{2,k/2}) \quad (70)$$

where  $F_2 = \begin{bmatrix} 1 & 1 \\ 1 & -1 \end{bmatrix}$  so that  $B_{2,k} = \begin{bmatrix} I_{k/2} & \Omega_{2,k/2} \\ I_{k/2} & -\Omega_{2,k/2} \end{bmatrix}$ .

Then, for all  $x \in \mathbb{C}^k$ , as we let  $z_i := x_{(i-1)k/2+1:ik/2}$  for  $i = 1, 2$ , we obtain

$$B_{2,k}x = \begin{bmatrix} z_1 + \Omega_{2,k/2}z_2 \\ z_1 - \Omega_{2,k/2}z_2 \end{bmatrix}. \quad (71)$$

We then let  $\tau := \Omega_{2,k/2}z_2$  so that

$$B_{2,k}x = \begin{bmatrix} z_1 + \tau \\ z_1 - \tau \end{bmatrix}. \quad (72)$$

This leads to Algo. 10 for the computation of  $x \mapsto A_{2,n}x$ .

---

**Algorithm 10** Butterfly kernel of radix-2
 

---

**Input:**  $x \in \mathbb{C}^n$ ,  $n = 2^t$   
**Output:**  $x := A_{2,n}x$

```

1: for  $q = 1, \dots, t$  do
2:    $k := 2^q$ 
3:    $n_b := n/k$ 
4:    $\ell := k/2$ 
5:   for  $b = 1, \dots, n_b$  do
6:     for  $j = 1, \dots, \ell$  do
7:        $\tau := \omega_k^{j-1} x_{(b-1)k+j+\ell}$ 
8:        $x_{(b-1)k+j+\ell} := x_{(b-1)k+j} - \tau$ 
9:        $x_{(b-1)k+j} := x_{(b-1)k+j} + \tau$ 
10:    end for
11:  end for
12: end for
13: return  $x$ 

```

---

The radix-2 conjugate butterfly kernel relies on the expression

$$\overline{B_{2,k}}x = \begin{bmatrix} z_1 + \overline{\Omega_{2,k/2}z_2} \\ z_1 - \overline{\Omega_{2,k/2}z_2} \end{bmatrix} \quad (73)$$

so that, as we let  $\tau := \overline{\Omega_{2,k/2}z_2}$ , we still have

$$\overline{B_{2,k}}x = \begin{bmatrix} z_1 + \tau \\ z_1 - \tau \end{bmatrix}. \quad (74)$$

This leads to Algo. 11 for the computation of  $x \mapsto \overline{A_{2,n}}x$ .

---

**Algorithm 11** Conjugate butterfly kernel of radix-2
 

---

**Input:**  $x \in \mathbb{C}^n$ ,  $n = 2^t$   
**Output:**  $x := \overline{A_{2,n}}x$

```

1: for  $q = 1, \dots, t$  do
2:    $k := 2^q$ 
3:    $n_b := n/k$ 
4:    $\ell := k/2$ 
5:   for  $b = 1, \dots, n_b$  do
6:     for  $j = 1, \dots, \ell$  do
7:        $\tau := \omega_k^{j-1} x_{(b-1)k+j+\ell}$ 
8:        $x_{(b-1)k+j+\ell} := x_{(b-1)k+j} - \tau$ 
9:        $x_{(b-1)k+j} := x_{(b-1)k+j} + \tau$ 
10:    end for
11:  end for
12: end for
13: return  $x$ 

```

---

On the other hand, we also have

$$B_{2,k}^T x = \begin{bmatrix} z_1 + z_2 \\ \Omega_{2,k/2} z_1 - \Omega_{2,k/2} z_2 \end{bmatrix} \quad (75)$$

so that if we let  $\tau := z_2$ , we obtain

$$B_{2,k}^T x = \begin{bmatrix} z_1 + \tau \\ \Omega_{2,k/2} (z_1 - \tau) \end{bmatrix}. \quad (76)$$

This leads to Algo. 12 for the computation of  $x \mapsto A_{2,n}^T x$ .

---

**Algorithm 12** Transposed butterfly kernel of radix-2

---

**Input:**  $x \in \mathbb{C}^n$ ,  $n = 2^t$

**Output:**  $x := A_{2,n}^T x$

```

1: for  $q = t, \dots, 1$  do
2:    $k := 2^q$ 
3:    $n_b := n/k$ 
4:    $\ell := k/2$ 
5:   for  $b = 1, \dots, n_b$  do
6:     for  $j = 1, \dots, \ell$  do
7:        $\tau := x_{(b-1)k+j+\ell}$ 
8:        $x_{(b-1)k+j+\ell} := \omega_k^{j-1} (x_{(b-1)k+j} - \tau)$ 
9:        $x_{(b-1)k+j} := x_{(b-1)k+j} + \tau$ 
10:    end for
11:  end for
12: end for
13: return  $x$ 

```

---

## A.2 Radix-4 butterfly-related kernels

For the radix-4 case, we have

$$B_{4,k} = (F_4 \otimes I_{k/4}) \text{diag} \left( I_{k/4}, \Omega_{4,k/4}, \Omega_{4,k/4}^2, \Omega_{4,k/4}^3 \right) \quad (77)$$

where

$$F_4 = \begin{bmatrix} 1 & 1 & 1 & 1 \\ 1 & -i & -1 & i \\ 1 & -1 & 1 & -1 \\ 1 & i & -1 & -i \end{bmatrix} \quad (78)$$

so that

$$B_{4,k} = \begin{bmatrix} I_{k/4} & \Omega_{4,k/4} & \Omega_{4,k/4}^2 & \Omega_{4,k/4}^3 \\ I_{k/4} & -i \cdot \Omega_{4,k/4} & -\Omega_{4,k/4}^2 & i \cdot \Omega_{4,k/4}^3 \\ I_{k/4} & -\Omega_{4,k/4} & \Omega_{4,k/4}^2 & -\Omega_{4,k/4}^3 \\ I_{k/4} & i \cdot \Omega_{4,k/4} & -\Omega_{4,k/4}^2 & -i \cdot \Omega_{4,k/4}^3 \end{bmatrix}. \quad (79)$$

Then, for all  $x \in \mathbb{C}^k$ , as we let  $z_i := x_{(i-1)k/4+1:ik/4}$  for  $i = 1, \dots, 4$ , we obtain

$$B_{4,k}x = \begin{bmatrix} z_1 + \Omega_{4,k/4}z_2 + \Omega_{4,k/4}^2z_3 + \Omega_{4,k/4}^3z_4 \\ z_1 - i \cdot \Omega_{4,k/4}z_2 - \Omega_{4,k/4}^2z_3 + i \cdot \Omega_{4,k/4}^3z_4 \\ z_1 - \Omega_{4,k/4}z_2 + \Omega_{4,k/4}^2z_3 - \Omega_{4,k/4}^3z_4 \\ z_1 + i \cdot \Omega_{4,k/4}z_2 - \Omega_{4,k/4}^2z_3 - i \cdot \Omega_{4,k/4}^3z_4 \end{bmatrix}. \quad (80)$$

Once we introduce

$$\begin{aligned} \tau_1 &:= z_1 + \Omega_{4,k/4}^2z_3, & \tau_2 &:= z_1 - \Omega_{4,k/4}^2z_3 \\ \tau_3 &:= \Omega_{4,k/4}z_2 + \Omega_{4,k/4}^3z_4, & \tau_4 &:= \Omega_{4,k/4}z_2 - \Omega_{4,k/4}^3z_4 \end{aligned} \quad (81)$$

we get

$$B_{4,k}x = \begin{bmatrix} \tau_1 + \tau_3 \\ \tau_2 - i \cdot \tau_4 \\ \tau_1 - \tau_3 \\ \tau_2 + i \cdot \tau_4 \end{bmatrix}. \quad (82)$$

This leads to Algo. 13 for the computation of  $x \mapsto A_{4,n}x$ .

---

**Algorithm 13** Butterfly kernel of radix-4

---

**Input:**  $x \in \mathbb{C}^n$ ,  $n = 4^t$

**Output:**  $x := A_{4,n}x$

```

1: for  $q = 1, \dots, t$  do
2:    $k := 4^q$ 
3:    $n_b := n/k$ 
4:    $\ell := k/4$ 
5:   for  $b = 1, \dots, n_b$  do
6:     for  $j = 1 \dots, \ell$  do
7:        $z_1 := x_{(b-1)k+j}$ 
8:        $z_2 := \omega_k^{j-1} x_{(b-1)k+\ell+j}$ 
9:        $z_3 := \omega_k^{2(j-1)} x_{(b-1)k+2\ell+j}$ 
10:       $z_4 := \omega_k^{3(j-1)} x_{(b-1)k+3\ell+j}$ 
11:       $\tau_1 := z_1 + z_3, \tau_2 := z_1 - z_3$ 
12:       $\tau_3 := z_2 + z_4, \tau_4 := z_2 - z_4$ 
13:       $x_{(b-1)k+j} := \tau_1 + \tau_3$ 
14:       $x_{(b-1)k+\ell+j} := \tau_2 - i \cdot \tau_4$ 
15:       $x_{(b-1)k+2\ell+j} := \tau_1 - \tau_3$ 
16:       $x_{(b-1)k+3\ell+j} := \tau_2 + i \cdot \tau_4$ 
17:     end for
18:   end for
19: end for
20: return  $x$ 

```

---

The radix-4 conjugate butterfly kernel relies on the expression

$$\overline{B_{4,k}x} = \begin{bmatrix} z_1 + \overline{\Omega_{4,k/4}z_2} + \overline{\Omega_{4,k/4}^2z_3} + \overline{\Omega_{4,k/4}^3z_4} \\ z_1 + i \cdot \overline{\Omega_{4,k/4}z_2} - \overline{\Omega_{4,k/4}^2z_3} - i \cdot \overline{\Omega_{4,k/4}^3z_4} \\ z_1 - \overline{\Omega_{4,k/4}z_2} + \overline{\Omega_{4,k/4}^2z_3} - \overline{\Omega_{4,k/4}^3z_4} \\ z_1 - i \cdot \overline{\Omega_{4,k/4}z_2} - \overline{\Omega_{4,k/4}^2z_3} + i \cdot \overline{\Omega_{4,k/4}^3z_4} \end{bmatrix} \quad (83)$$

so that, as we introduce

$$\begin{aligned} \tau_1 &:= z_1 + \overline{\Omega_{4,k/4}^2z_3}, & \tau_2 &:= z_1 - \overline{\Omega_{4,k/4}^2z_3} \\ \tau_3 &:= \overline{\Omega_{4,k/4}z_2} + \overline{\Omega_{4,k/4}^3z_4}, & \tau_4 &:= \overline{\Omega_{4,k/4}z_2} - \overline{\Omega_{4,k/4}^3z_4} \end{aligned} \quad (84)$$

we get

$$\overline{B_{4,k}x} = \begin{bmatrix} \tau_1 + \tau_3 \\ \tau_2 + i \cdot \tau_4 \\ \tau_1 - \tau_3 \\ \tau_2 - i \cdot \tau_4 \end{bmatrix}. \quad (85)$$

This leads to Algo. 14 for the computation of  $x \mapsto \overline{A_{4,n}x}$ .

---

**Algorithm 14** Conjugate butterfly kernel of radix-4

---

**Input:**  $x \in \mathbb{C}^n, n = 4^t$

**Output:**  $x := \overline{A_{4,n}x}$

```

1: for  $q = 1, \dots, t$  do
2:    $k := 4^q$ 
3:    $n_b := n/k$ 
4:    $\ell := k/4$ 
5:   for  $b = 1, \dots, n_b$  do
6:     for  $j = 1, \dots, \ell$  do
7:        $z_1 := \overline{x_{(b-1)k+j}}$ 
8:        $z_2 := \overline{\omega_k^{j-1} x_{(b-1)k+\ell+j}}$ 
9:        $z_3 := \overline{\omega_k^{2(j-1)} x_{(b-1)k+2\ell+j}}$ 
10:       $z_4 := \overline{\omega_k^{3(j-1)} x_{(b-1)k+3\ell+j}}$ 
11:       $\tau_1 := z_1 + z_3, \tau_2 := z_1 - z_3$ 
12:       $\tau_3 := z_2 + z_4, \tau_4 := z_2 - z_4$ 
13:       $x_{(b-1)k+j} := \tau_1 + \tau_3$ 
14:       $x_{(b-1)k+\ell+j} := \tau_2 + i \cdot \tau_4$ 
15:       $x_{(b-1)k+2\ell+j} := \tau_1 - \tau_3$ 
16:       $x_{(b-1)k+3\ell+j} := \tau_2 - i \cdot \tau_4$ 
17:     end for
18:   end for
19: end for
20: return  $x$ 
```

---

The radix-4 transposed butterfly kernel relies on the expression

$$B_{4,k}^T x = \begin{bmatrix} z_1 + z_2 + z_3 + z_4 \\ \Omega_{4,k/4} z_1 - i \cdot \Omega_{4,k/4} z_2 - \Omega_{4,k/4} z_3 + i \cdot \Omega_{4,k/4} z_4 \\ \Omega_{4,k/4}^2 z_1 - \Omega_{4,k/4}^2 z_2 + \Omega_{4,k/4}^2 z_3 - \Omega_{4,k/4}^2 z_4 \\ \Omega_{4,k/4}^3 z_1 + i \cdot \Omega_{4,k/4}^3 z_2 - \Omega_{4,k/4}^3 z_3 - i \cdot \Omega_{4,k/4}^3 z_4 \end{bmatrix}. \quad (86)$$

As we introduce

$$\begin{aligned} \tau_1 &:= z_1 + z_3, & \tau_2 &:= \Omega_{4,k/4}(z_1 - z_3) \\ \tau_3 &:= z_2 + z_4, & \tau_4 &:= \Omega_{4,k/4}(z_2 - z_4) \end{aligned} \quad (87)$$

we obtain

$$B_{4,k}^T x = \begin{bmatrix} \tau_1 + \tau_3 \\ \tau_2 - i \cdot \tau_4 \\ \Omega_{4,k/4}^2(\tau_1 - \tau_3) \\ \Omega_{4,k/4}^2(\tau_2 + i \cdot \tau_4) \end{bmatrix}. \quad (88)$$

This leads to Algo. 15 for the computation of  $x \mapsto A_{4,n}^T x$ .

---

**Algorithm 15** Transposed butterfly kernel of radix-4

---

**Input:**  $x \in \mathbb{C}^n$ ,  $n = 4^t$

**Output:**  $x := A_{4,n}^T x$

```

1: for  $q = t, \dots, 1$  do
2:    $k := 4^q$ 
3:    $n_b := n/k$ 
4:    $\ell := k/4$ 
5:   for  $b = 1, \dots, n_b$  do
6:     for  $j = 1 \dots, \ell$  do
7:        $z_1 := x_{(b-1)k+j}$ 
8:        $z_2 := x_{(b-1)k+\ell+j}$ 
9:        $z_3 := x_{(b-1)k+2\ell+j}$ 
10:       $z_4 := x_{(b-1)k+3\ell+j}$ 
11:       $\tau_1 := z_1 + z_3, \tau_2 := \omega_k^{j-1}(z_1 - z_3)$ 
12:       $\tau_3 := z_2 + z_4, \tau_4 := \omega_k^{j-1}(z_2 - z_4)$ 
13:       $x_{(b-1)k+j} := \tau_1 + \tau_3$ 
14:       $x_{(b-1)k+\ell+j} := \tau_2 - i \cdot \tau_4$ 
15:       $x_{(b-1)k+2\ell+j} := \omega_k^{2(j-1)}(\tau_1 - \tau_3)$ 
16:       $x_{(b-1)k+3\ell+j} := \omega_k^{2(j-1)}(\tau_2 + i \cdot \tau_4)$ 
17:    end for
18:  end for
19: end for
20: return  $x$ 
```

---

### A.3 Radix-8 butterfly-related kernels

For the radix-8 case, we have

$$B_{8,k} = (F_8 \otimes I_{k/8}) \text{diag} \left( I_{k/8}, \Omega_{8,k/8}, \Omega_{8,k/8}^2, \Omega_{8,k/8}^3, \Omega_{8,k/8}^4, \Omega_{8,k/8}^5, \Omega_{8,k/8}^6, \Omega_{8,k/8}^7 \right) \quad (89)$$



where

$$F_8 = \begin{bmatrix} 1 & 1 & 1 & 1 & 1 & 1 & 1 & 1 \\ 1 & a & -i & b & -1 & -a & i & -b \\ 1 & -i & -1 & i & 1 & -i & -1 & i \\ 1 & b & i & a & -1 & -b & -i & -a \\ 1 & -1 & 1 & -1 & 1 & -1 & 1 & -1 \\ 1 & -a & -i & -b & -1 & a & i & b \\ 1 & i & -1 & -i & 1 & i & -1 & -i \\ 1 & -b & i & -a & -1 & b & -i & a \end{bmatrix} \quad (90)$$

in which  $a = (1 - i)/\sqrt{2}$  and  $b = -(1 + i)/\sqrt{2} = -ia$ , so that

$$B_{8,k} = \begin{bmatrix} I_{k/8} & \Omega_{8,k/8} & \Omega_{8,k/8}^2 & \Omega_{8,k/8}^3 & \Omega_{8,k/8}^4 & \Omega_{8,k/8}^5 & \Omega_{8,k/8}^6 & \Omega_{8,k/8}^7 \\ I_{k/8} & a \cdot \Omega_{8,k/8} & -i \cdot \Omega_{8,k/8}^2 & b \cdot \Omega_{8,k/8}^3 & -\Omega_{8,k/8}^4 & -a \cdot \Omega_{8,k/8}^5 & i \cdot \Omega_{8,k/8}^6 & -b \cdot \Omega_{8,k/8}^7 \\ I_{k/8} & -i \cdot \Omega_{8,k/8} & -\Omega_{8,k/8}^2 & i \cdot \Omega_{8,k/8}^3 & \Omega_{8,k/8}^4 & -i \cdot \Omega_{8,k/8}^5 & -\Omega_{8,k/8}^6 & i \cdot \Omega_{8,k/8}^7 \\ I_{k/8} & b \cdot \Omega_{8,k/8} & i \cdot \Omega_{8,k/8}^2 & a \cdot \Omega_{8,k/8}^3 & -\Omega_{8,k/8}^4 & -b \cdot \Omega_{8,k/8}^5 & -i \cdot \Omega_{8,k/8}^6 & -a \cdot \Omega_{8,k/8}^7 \\ I_{k/8} & -\Omega_{8,k/8} & \Omega_{8,k/8}^2 & -\Omega_{8,k/8}^3 & \Omega_{8,k/8}^4 & -\Omega_{8,k/8}^5 & \Omega_{8,k/8}^6 & -\Omega_{8,k/8}^7 \\ I_{k/8} & -a \cdot \Omega_{8,k/8} & -i \cdot \Omega_{8,k/8}^2 & -b \cdot \Omega_{8,k/8}^3 & -\Omega_{8,k/8}^4 & a \cdot \Omega_{8,k/8}^5 & i \cdot \Omega_{8,k/8}^6 & b \cdot \Omega_{8,k/8}^7 \\ I_{k/8} & i \cdot \Omega_{8,k/8} & -\Omega_{8,k/8}^2 & -i \cdot \Omega_{8,k/8}^3 & \Omega_{8,k/8}^4 & i \cdot \Omega_{8,k/8}^5 & -\Omega_{8,k/8}^6 & -i \cdot \Omega_{8,k/8}^7 \\ I_{k/8} & -b \cdot \Omega_{8,k/8} & i \cdot \Omega_{8,k/8}^2 & -a \cdot \Omega_{8,k/8}^3 & -\Omega_{8,k/8}^4 & b \cdot \Omega_{8,k/8}^5 & -i \cdot \Omega_{8,k/8}^6 & a \cdot \Omega_{8,k/8}^7 \end{bmatrix}. \quad (91)$$

Then, for all  $x \in \mathbb{C}^k$ , as we let  $z_i := x_{(i-1)k/8+1:ik/8}$  for  $i = 1, \dots, 8$ , we have

$$B_{8,k}x = \begin{bmatrix} z_1 + \Omega_{8,k/8}z_2 + \Omega_{8,k/8}^2z_3 + \Omega_{8,k/8}^3z_4 + \Omega_{8,k/8}^4z_5 + \Omega_{8,k/8}^5z_6 + \Omega_{8,k/8}^6z_7 + \Omega_{8,k/8}^7z_8 \\ z_1 + a \cdot \Omega_{8,k/8}z_2 - i \cdot \Omega_{8,k/8}^2z_3 + b \cdot \Omega_{8,k/8}^3z_4 - \Omega_{8,k/8}^4z_5 - a \cdot \Omega_{8,k/8}^5z_6 + i \cdot \Omega_{8,k/8}^6z_7 - b \cdot \Omega_{8,k/8}^7z_8 \\ z_1 - i \cdot \Omega_{8,k/8}z_2 - \Omega_{8,k/8}^2z_3 + i \cdot \Omega_{8,k/8}^3z_4 + \Omega_{8,k/8}^4z_5 - i \cdot \Omega_{8,k/8}^5z_6 - \Omega_{8,k/8}^6z_7 + i \cdot \Omega_{8,k/8}^7z_8 \\ z_1 + b \cdot \Omega_{8,k/8}z_2 + i \cdot \Omega_{8,k/8}^2z_3 + a \cdot \Omega_{8,k/8}^3z_4 - \Omega_{8,k/8}^4z_5 - b \cdot \Omega_{8,k/8}^5z_6 - i \cdot \Omega_{8,k/8}^6z_7 - a \cdot \Omega_{8,k/8}^7z_8 \\ z_1 - \Omega_{8,k/8}z_2 + \Omega_{8,k/8}^2z_3 - \Omega_{8,k/8}^3z_4 + \Omega_{8,k/8}^4z_5 - \Omega_{8,k/8}^5z_6 + \Omega_{8,k/8}^6z_7 - \Omega_{8,k/8}^7z_8 \\ z_1 - a \cdot \Omega_{8,k/8}z_2 - i \cdot \Omega_{8,k/8}^2z_3 - b \cdot \Omega_{8,k/8}^3z_4 - \Omega_{8,k/8}^4z_5 + a \cdot \Omega_{8,k/8}^5z_6 + i \cdot \Omega_{8,k/8}^6z_7 + b \cdot \Omega_{8,k/8}^7z_8 \\ z_1 + i \cdot \Omega_{8,k/8}z_2 - \Omega_{8,k/8}^2z_3 - i \cdot \Omega_{8,k/8}^3z_4 + \Omega_{8,k/8}^4z_5 + i \cdot \Omega_{8,k/8}^5z_6 - \Omega_{8,k/8}^6z_7 - i \cdot \Omega_{8,k/8}^7z_8 \\ z_1 - b \cdot \Omega_{8,k/8}z_2 + i \cdot \Omega_{8,k/8}^2z_3 - a \cdot \Omega_{8,k/8}^3z_4 - \Omega_{8,k/8}^4z_5 + b \cdot \Omega_{8,k/8}^5z_6 - i \cdot \Omega_{8,k/8}^6z_7 + a \cdot \Omega_{8,k/8}^7z_8 \end{bmatrix}. \quad (92)$$

As we introduce

$$\begin{aligned} \tau_1 &:= z_1 + \Omega_{8,k/8}^4z_5, & \tau_2 &:= z_1 - \Omega_{8,k/8}^4z_5 \\ \tau_3 &:= \Omega_{8,k/8}z_2 + \Omega_{8,k/8}^5z_6, & \tau_4 &:= \Omega_{8,k/8}z_2 - \Omega_{8,k/8}^5z_6 \\ \tau_5 &:= \Omega_{8,k/8}^2z_3 + \Omega_{8,k/8}^6z_7, & \tau_6 &:= \Omega_{8,k/8}^2z_3 - \Omega_{8,k/8}^6z_7 \\ \tau_7 &:= \Omega_{8,k/8}^3z_4 + \Omega_{8,k/8}^7z_8, & \tau_8 &:= \Omega_{8,k/8}^3z_4 - \Omega_{8,k/8}^7z_8 \end{aligned} \quad (93)$$

we obtain

$$B_{8,k}x = \begin{bmatrix} \tau_1 + \tau_3 + \tau_5 + \tau_7 \\ \tau_2 + a \cdot \tau_4 - i \cdot \tau_6 + b \cdot \tau_8 \\ \tau_1 - i \cdot \tau_3 - \tau_5 + i \cdot \tau_7 \\ \tau_2 + b \cdot \tau_4 + i \cdot \tau_6 + a \cdot \tau_8 \\ \tau_1 - \tau_3 + \tau_5 - \tau_7 \\ \tau_2 - a \cdot \tau_4 - i \cdot \tau_6 - b \cdot \tau_8 \\ \tau_1 + i \cdot \tau_3 - \tau_5 - i \cdot \tau_7 \\ \tau_2 - b \cdot \tau_4 + i \cdot \tau_6 - a \cdot \tau_8 \end{bmatrix}. \quad (94)$$

This leads to Algo. 16 for the computation of  $x \mapsto A_{8,n}x$ .

---

**Algorithm 16** Butterfly kernel of radix-8

---

**Input:**  $x \in \mathbb{C}^n$ ,  $n = 8^t$

**Output:**  $x := A_{8,n}x$

```

1: for  $q = 1, \dots, t$  do
2:    $k := 8^q$ 
3:    $n_b := n/k$ 
4:    $\ell := k/8$ 
5:   for  $b = 1, \dots, n_b$  do
6:     for  $j = 1 \dots, \ell$  do
7:        $z_1 := x_{(b-1)k+j}$ 
8:        $z_2 := \omega_k^{j-1} x_{(b-1)k+\ell+j}$ 
9:        $z_3 := \omega_k^{2(j-1)} x_{(b-1)k+2\ell+j}$ 
10:       $z_4 := \omega_k^{3(j-1)} x_{(b-1)k+3\ell+j}$ 
11:       $z_5 := \omega_k^{4(j-1)} x_{(b-1)k+4\ell+j}$ 
12:       $z_6 := \omega_k^{5(j-1)} x_{(b-1)k+5\ell+j}$ 
13:       $z_7 := \omega_k^{6(j-1)} x_{(b-1)k+6\ell+j}$ 
14:       $z_8 := \omega_k^{7(j-1)} x_{(b-1)k+7\ell+j}$ 
15:       $\tau_1 := z_1 + z_5, \tau_2 := z_1 - z_5$ 
16:       $\tau_3 := z_2 + z_6, \tau_4 := z_2 - z_6$ 
17:       $\tau_5 := z_3 + z_7, \tau_6 := z_3 - z_7$ 
18:       $\tau_7 := z_4 + z_8, \tau_8 := z_4 - z_8$ 
19:       $x_{(b-1)k+j} := \tau_1 + \tau_3 + \tau_5 + \tau_7$ 
20:       $x_{(b-1)k+\ell+j} := \tau_2 + a \cdot \tau_4 - i \cdot \tau_6 + b \cdot \tau_8$ 
21:       $x_{(b-1)k+2\ell+j} := \tau_1 - i \cdot \tau_3 - \tau_5 + i \cdot \tau_7$ 
22:       $x_{(b-1)k+3\ell+j} := \tau_2 + b \cdot \tau_4 + i \cdot \tau_6 + a \cdot \tau_8$ 
23:       $x_{(b-1)k+4\ell+j} := \tau_1 - \tau_3 + \tau_5 - \tau_7$ 
24:       $x_{(b-1)k+5\ell+j} := \tau_2 - a \cdot \tau_4 - i \cdot \tau_6 - b \cdot \tau_8$ 
25:       $x_{(b-1)k+6\ell+j} := \tau_1 + i \cdot \tau_3 - \tau_5 - i \cdot \tau_7$ 
26:       $x_{(b-1)k+7\ell+j} := \tau_2 - b \cdot \tau_4 + i \cdot \tau_6 - a \cdot \tau_8$ 
27:     end for
28:   end for
29: end for
30: return  $x$ 

```

---

The radix-8 conjugate butterfly kernel relies on the expression

$$\overline{B_{8,k}x} = \begin{bmatrix} z_1 + \overline{\Omega_{8,k/8} z_2} + \overline{\Omega_{8,k/8}^2 z_3} + \overline{\Omega_{8,k/8}^3 z_4} + \overline{\Omega_{8,k/8}^4 z_5} + \overline{\Omega_{8,k/8}^5 z_6} + \overline{\Omega_{8,k/8}^6 z_7} + \overline{\Omega_{8,k/8}^7 z_8} \\ z_1 + \overline{a \cdot \Omega_{8,k/8} z_2} + i \cdot \overline{\Omega_{8,k/8}^2 z_3} + \overline{b \cdot \Omega_{8,k/8}^3 z_4} - \overline{\Omega_{8,k/8}^4 z_5} - \overline{a \cdot \Omega_{8,k/8}^5 z_6} - i \cdot \overline{\Omega_{8,k/8}^6 z_7} - \overline{b \cdot \Omega_{8,k/8}^7 z_8} \\ z_1 + i \cdot \overline{\Omega_{8,k/8} z_2} - \overline{\Omega_{8,k/8}^2 z_3} - i \cdot \overline{\Omega_{8,k/8}^3 z_4} + \overline{\Omega_{8,k/8}^4 z_5} + i \cdot \overline{\Omega_{8,k/8}^5 z_6} - \overline{\Omega_{8,k/8}^6 z_7} - i \cdot \overline{\Omega_{8,k/8}^7 z_8} \\ z_1 + \overline{b \cdot \Omega_{8,k/8} z_2} - i \cdot \overline{\Omega_{8,k/8}^2 z_3} + \overline{a \cdot \Omega_{8,k/8}^3 z_4} - \overline{\Omega_{8,k/8}^4 z_5} - \overline{b \cdot \Omega_{8,k/8}^5 z_6} + i \cdot \overline{\Omega_{8,k/8}^6 z_7} - \overline{a \cdot \Omega_{8,k/8}^7 z_8} \\ z_1 - \overline{\Omega_{8,k/8} z_2} + \overline{\Omega_{8,k/8}^2 z_3} - \overline{\Omega_{8,k/8}^3 z_4} + \overline{\Omega_{8,k/8}^4 z_5} - \overline{\Omega_{8,k/8}^5 z_6} + \overline{\Omega_{8,k/8}^6 z_7} - \overline{\Omega_{8,k/8}^7 z_8} \\ z_1 - \overline{a \cdot \Omega_{8,k/8} z_2} + i \cdot \overline{\Omega_{8,k/8}^2 z_3} - \overline{b \cdot \Omega_{8,k/8}^3 z_4} - \overline{\Omega_{8,k/8}^4 z_5} + \overline{a \cdot \Omega_{8,k/8}^5 z_6} - i \cdot \overline{\Omega_{8,k/8}^6 z_7} + \overline{b \cdot \Omega_{8,k/8}^7 z_8} \\ z_1 - i \cdot \overline{\Omega_{8,k/8} z_2} - \overline{\Omega_{8,k/8}^2 z_3} + i \cdot \overline{\Omega_{8,k/8}^3 z_4} + \overline{\Omega_{8,k/8}^4 z_5} - i \cdot \overline{\Omega_{8,k/8}^5 z_6} - \overline{\Omega_{8,k/8}^6 z_7} + i \cdot \overline{\Omega_{8,k/8}^7 z_8} \\ z_1 - \overline{b \cdot \Omega_{8,k/8} z_2} - i \cdot \overline{\Omega_{8,k/8}^2 z_3} - \overline{a \cdot \Omega_{8,k/8}^3 z_4} - \overline{\Omega_{8,k/8}^4 z_5} + \overline{b \cdot \Omega_{8,k/8}^5 z_6} + i \cdot \overline{\Omega_{8,k/8}^6 z_7} + \overline{a \cdot \Omega_{8,k/8}^7 z_8} \end{bmatrix} \quad (95)$$

so that, as we introduce

$$\begin{aligned} \tau_1 &:= z_1 + \overline{\Omega_{8,k/8}^4 z_5}, & \tau_2 &:= z_1 - \overline{\Omega_{8,k/8}^4 z_5} \\ \tau_3 &:= \overline{\Omega_{8,k/8} z_2} + \overline{\Omega_{8,k/8}^5 z_6}, & \tau_4 &:= \overline{\Omega_{8,k/8} z_2} - \overline{\Omega_{8,k/8}^5 z_6} \\ \tau_5 &:= \overline{\Omega_{8,k/8}^2 z_3} + \overline{\Omega_{8,k/8}^6 z_7}, & \tau_6 &:= \overline{\Omega_{8,k/8}^2 z_3} - \overline{\Omega_{8,k/8}^6 z_7} \\ \tau_7 &:= \overline{\Omega_{8,k/8}^3 z_4} + \overline{\Omega_{8,k/8}^7 z_8}, & \tau_8 &:= \overline{\Omega_{8,k/8}^3 z_4} - \overline{\Omega_{8,k/8}^7 z_8} \end{aligned} \quad (96)$$

we obtain

$$\overline{B_{8,k}x} = \begin{bmatrix} \tau_1 + \tau_3 + \tau_5 + \tau_7 \\ \tau_2 + \overline{a \cdot \tau_4} + i \cdot \tau_6 + \overline{b \cdot \tau_8} \\ \tau_1 + i \cdot \tau_3 - \tau_5 - i \cdot \tau_7 \\ \tau_2 + \overline{b \cdot \tau_4} - i \cdot \tau_6 + \overline{a \cdot \tau_8} \\ \tau_1 - \tau_3 + \tau_5 - \tau_7 \\ \tau_2 - \overline{a \cdot \tau_4} + i \cdot \tau_6 - \overline{b \cdot \tau_8} \\ \tau_1 - i \cdot \tau_3 - \tau_5 + i \cdot \tau_7 \\ \tau_2 - \overline{b \cdot \tau_4} - i \cdot \tau_6 - \overline{a \cdot \tau_8} \end{bmatrix}. \quad (97)$$

This leads to Algo. 17 for the computation of  $x \mapsto \overline{A_{8,n}x}$ .

---

**Algorithm 17** Conjugate butterfly kernel of radix-8
 

---

**Input:**  $x \in \mathbb{C}^n$ ,  $n = 8^t$ 
**Output:**  $x := A_{8,n}x$ 

```

1: for  $q = 1, \dots, t$  do
2:    $k := 8^q$ 
3:    $n_b := n/k$ 
4:    $\ell := k/8$ 
5:   for  $b = 1, \dots, n_b$  do
6:     for  $j = 1 \dots, \ell$  do
7:        $z_1 := x_{(b-1)k+j}$ 
8:        $z_2 := \omega_k^{j-1} x_{(b-1)k+\ell+j}$ 
9:        $z_3 := \omega_k^{2(j-1)} x_{(b-1)k+2\ell+j}$ 
10:       $z_4 := \omega_k^{3(j-1)} x_{(b-1)k+3\ell+j}$ 
11:       $z_5 := \omega_k^{4(j-1)} x_{(b-1)k+4\ell+j}$ 
12:       $z_6 := \omega_k^{5(j-1)} x_{(b-1)k+5\ell+j}$ 
13:       $z_7 := \omega_k^{6(j-1)} x_{(b-1)k+6\ell+j}$ 
14:       $z_8 := \omega_k^{7(j-1)} x_{(b-1)k+7\ell+j}$ 
15:       $\tau_1 := z_1 + z_5$ ,  $\tau_2 := z_1 - z_5$ 
16:       $\tau_3 := z_2 + z_6$ ,  $\tau_4 := z_2 - z_6$ 
17:       $\tau_5 := z_3 + z_7$ ,  $\tau_6 := z_3 - z_7$ 
18:       $\tau_7 := z_4 + z_8$ ,  $\tau_8 := z_4 - z_8$ 
19:       $x_{(b-1)k+j} := \tau_1 + \tau_3 + \tau_5 + \tau_7$ 
20:       $x_{(b-1)k+\ell+j} := \tau_2 + \bar{a} \cdot \tau_4 + i \cdot \tau_6 + \bar{b} \cdot \tau_8$ 
21:       $x_{(b-1)k+2\ell+j} := \tau_1 + i \cdot \tau_3 - \tau_5 - i \cdot \tau_7$ 
22:       $x_{(b-1)k+3\ell+j} := \tau_2 + \bar{b} \cdot \tau_4 - i \cdot \tau_6 + \bar{a} \cdot \tau_8$ 
23:       $x_{(b-1)k+4\ell+j} := \tau_1 - \tau_3 + \tau_5 - \tau_7$ 
24:       $x_{(b-1)k+5\ell+j} := \tau_2 - \bar{a} \cdot \tau_4 + i \cdot \tau_6 - \bar{b} \cdot \tau_8$ 
25:       $x_{(b-1)k+6\ell+j} := \tau_1 - i \cdot \tau_3 - \tau_5 + i \cdot \tau_7$ 
26:       $x_{(b-1)k+7\ell+j} := \tau_2 - \bar{b} \cdot \tau_4 - i \cdot \tau_6 - \bar{a} \cdot \tau_8$ 
27:     end for
28:   end for
29: end for
30: return  $x$ 

```

---

On the other hand, we have

$$B_{8,k}^T x = \begin{bmatrix} z_1 + z_2 + z_3 + z_4 + z_5 + z_6 + z_7 + z_8 \\ \Omega_{8,k/8} z_1 + a \cdot \Omega_{8,k/8} z_2 - i \cdot \Omega_{8,k/8} z_3 + b \cdot \Omega_{8,k/8} z_4 - \Omega_{8,k/8} z_5 - a \cdot \Omega_{8,k/8} z_6 + i \cdot \Omega_{8,k/8} z_7 - b \cdot \Omega_{8,k/8} z_8 \\ \Omega_{8,k/8}^2 z_1 - i \cdot \Omega_{8,k/8}^2 z_2 - \Omega_{8,k/8}^2 z_3 + i \cdot \Omega_{8,k/8}^2 z_4 + \Omega_{8,k/8}^2 z_5 - i \cdot \Omega_{8,k/8}^2 z_6 - \Omega_{8,k/8}^2 z_7 + i \cdot \Omega_{8,k/8}^2 z_8 \\ \Omega_{8,k/8}^3 z_1 + b \cdot \Omega_{8,k/8}^3 z_2 + i \cdot \Omega_{8,k/8}^3 z_3 + a \cdot \Omega_{8,k/8}^3 z_4 - \Omega_{8,k/8}^3 z_5 - b \cdot \Omega_{8,k/8}^3 z_6 - i \cdot \Omega_{8,k/8}^3 z_7 - a \cdot \Omega_{8,k/8}^3 z_8 \\ \Omega_{8,k/8}^4 z_1 - \Omega_{8,k/8}^4 z_2 + \Omega_{8,k/8}^4 z_3 - \Omega_{8,k/8}^4 z_4 + \Omega_{8,k/8}^4 z_5 - \Omega_{8,k/8}^4 z_6 + \Omega_{8,k/8}^4 z_7 - \Omega_{8,k/8}^4 z_8 \\ \Omega_{8,k/8}^5 z_1 - a \cdot \Omega_{8,k/8}^5 z_2 - i \cdot \Omega_{8,k/8}^5 z_3 - b \cdot \Omega_{8,k/8}^5 z_4 - \Omega_{8,k/8}^5 z_5 + a \cdot \Omega_{8,k/8}^5 z_6 + i \cdot \Omega_{8,k/8}^5 z_7 + b \cdot \Omega_{8,k/8}^5 z_8 \\ \Omega_{8,k/8}^6 z_1 + i \cdot \Omega_{8,k/8}^6 z_2 - \Omega_{8,k/8}^6 z_3 - i \cdot \Omega_{8,k/8}^6 z_4 + \Omega_{8,k/8}^6 z_5 + i \cdot \Omega_{8,k/8}^6 z_6 - \Omega_{8,k/8}^6 z_7 - i \cdot \Omega_{8,k/8}^6 z_8 \\ \Omega_{8,k/8}^7 z_1 - b \cdot \Omega_{8,k/8}^7 z_2 + i \cdot \Omega_{8,k/8}^7 z_3 - a \cdot \Omega_{8,k/8}^7 z_4 - \Omega_{8,k/8}^7 z_5 + b \cdot \Omega_{8,k/8}^7 z_6 - i \cdot \Omega_{8,k/8}^7 z_7 + a \cdot \Omega_{8,k/8}^7 z_8 \end{bmatrix}. \quad (98)$$

As we introduce

$$\begin{aligned} \tau_1 &:= z_1 + z_5, & \tau_2 &:= \Omega_{8,k/8}(z_1 - z_5) \\ \tau_3 &:= z_2 + z_6, & \tau_4 &:= \Omega_{8,k/8}(z_2 - z_6) \\ \tau_5 &:= z_3 + z_7, & \tau_6 &:= \Omega_{8,k/8}(z_3 - z_7) \\ \tau_7 &:= z_4 + z_8, & \tau_8 &:= \Omega_{8,k/8}(z_4 - z_8) \end{aligned} \quad (99)$$

we obtain

$$B_{8,k}^T x = \begin{bmatrix} \tau_1 + \tau_3 + \tau_5 + \tau_7 \\ \tau_2 + a \cdot \tau_4 - i \cdot \tau_6 + b \cdot \tau_8 \\ \Omega_{8,k/8}^2(\tau_1 - i \cdot \tau_3 - \tau_5 + i \cdot \tau_7) \\ \Omega_{8,k/8}^2(\tau_2 + b \cdot \tau_4 + i \cdot \tau_6 + a \cdot \tau_8) \\ \Omega_{8,k/8}^4(\tau_1 - \tau_3 + \tau_5 - \tau_7) \\ \Omega_{8,k/8}^4(\tau_2 - a \cdot \tau_4 - i \cdot \tau_6 - b \cdot \tau_8) \\ \Omega_{8,k/8}^6(\tau_1 + i \cdot \tau_3 - \tau_5 - i \cdot \tau_7) \\ \Omega_{8,k/8}^6(\tau_2 - b \cdot \tau_4 + i \cdot \tau_6 - a \cdot \tau_8) \end{bmatrix}. \quad (100)$$

This leads to Algo. 18 for the computation of  $x \mapsto A_{8,n}^T x$ .

---

**Algorithm 18** Transposed butterfly kernel of radix-8
 

---

**Input:**  $x \in \mathbb{C}^n$ ,  $n = 8^t$ 
**Output:**  $x := A_{8,n}^T x$ 

```

1: for  $q = t, \dots, 1$  do
2:    $k := 8^q$ 
3:    $n_b := n/k$ 
4:    $\ell := k/8$ 
5:   for  $b = 1, \dots, n_b$  do
6:     for  $j = 1 \dots, \ell$  do
7:        $z_1 := x_{(b-1)k+j}$ 
8:        $z_2 := x_{(b-1)k+\ell+j}$ 
9:        $z_3 := x_{(b-1)k+2\ell+j}$ 
10:       $z_4 := x_{(b-1)k+3\ell+j}$ 
11:       $z_5 := x_{(b-1)k+4\ell+j}$ 
12:       $z_6 := x_{(b-1)k+5\ell+j}$ 
13:       $z_7 := x_{(b-1)k+6\ell+j}$ 
14:       $z_8 := x_{(b-1)k+7\ell+j}$ 
15:       $\tau_1 := z_1 + z_5$ ,  $\tau_2 := \omega_k^{j-1}(z_1 - z_5)$ 
16:       $\tau_3 := z_2 + z_6$ ,  $\tau_4 := \omega_k^{j-1}(z_2 - z_6)$ 
17:       $\tau_5 := z_3 + z_7$ ,  $\tau_6 := \omega_k^{j-1}(z_3 - z_7)$ 
18:       $\tau_7 := z_4 + z_8$ ,  $\tau_8 := \omega_k^{j-1}(z_4 - z_8)$ 
19:       $x_{(b-1)k+j} := \tau_1 + \tau_3 + \tau_5 + \tau_7$ 
20:       $x_{(b-1)k+\ell+j} := \tau_2 + a \cdot \tau_4 - i \cdot \tau_6 + b \cdot \tau_8$ 
21:       $x_{(b-1)k+2\ell+j} := \omega_k^{2(j-1)}(\tau_1 - i \cdot \tau_3 - \tau_5 + i \cdot \tau_7)$ 
22:       $x_{(b-1)k+3\ell+j} := \omega_k^{2(j-1)}(\tau_2 + b \cdot \tau_4 + i \cdot \tau_6 + a \cdot \tau_8)$ 
23:       $x_{(b-1)k+4\ell+j} := \omega_k^{4(j-1)}(\tau_1 - \tau_3 + \tau_5 - \tau_7)$ 
24:       $x_{(b-1)k+5\ell+j} := \omega_k^{4(j-1)}(\tau_2 - a \cdot \tau_4 - i \cdot \tau_6 - b \cdot \tau_8)$ 
25:       $x_{(b-1)k+6\ell+j} := \omega_k^{6(j-1)}(\tau_1 + i \cdot \tau_3 - \tau_5 - i \cdot \tau_7)$ 
26:       $x_{(b-1)k+7\ell+j} := \omega_k^{6(j-1)}(\tau_2 - b \cdot \tau_4 + i \cdot \tau_6 - a \cdot \tau_8)$ 
27:     end for
28:   end for
29: end for
30: return  $x$ 

```

---